2010

Pyridoxal Kinase: Its Role in Vitamin B6 Metabolism

Jigarkumar Desai
Virginia Commonwealth University

PYRIDOXAL KINASE (PL KINASE): ROLE IN VITAMIN B_6 METABOLISM

A dissertation submitted in partial fulfillment of the requirements for the degree of M.S. at Virginia Commonwealth University.

by

JIGARKUMAR VINODBHAI DESAI
Bachelors of Pharmacy, The Maharaja Sayajirao University of Baroda, India, 2008

DIRECTOR: DR. MARTIN SAFO, Ph. D.
ASSOCIATE PROFESSOR, DEPARTMENT OF MEDICINAL CHEMISTRY

Virginia Commonwealth University
Richmond, Virginia
July, 2010

Acknowledgement

I am deeply indebted to my advisor, Dr. Martin Safo, for his constant support and encouragement, without which this research would not have been possible. His cordial and considerate attitude, suggestions and cooperation right from the inception of this project have been very valuable. He has been a constant source of inspiration and encouragement.

I feel at a loss of words while expressing my gratitude to Dr. Mohini Ghatge. Her scholastic approach, meticulous supervision and constructive criticism have been the major guiding force that helped me accomplish this task. I shall forever value her words of wisdom. I am also grateful to Dr. Faik Musayev for teaching me the tricks and techniques of X-ray crystallography.

I am very much thankful to Dr. Umesh Desai and Dr. Darrel Peterson for agreeing to be in my advisory committee. I am grateful to them for their valuable advice on enzyme kinetics and protein purification.

Working in Institute of Structural Biology and Drug Discovery for one and a half years has been a superb experience and I will always cherish every moment spent in the institute. I would like to thank all my friends at the institute and in Medicinal Chemistry for being supportive.

I would like to mention all my friends here in Richmond and outside the city for their constant words of encouragement and for believing in me. I would like to thank my family members, without whom I would not have achieved this.

Last but not the least I would like to thank Department of Medicinal Chemistry at VCU for giving me this opportunity.

Table of Contents

Page

List of Tables

Page

List of Figures

Page

Abstract

PYRIDOXAL KINASE (PL KINASE): ROLE IN VITAMIN B_6 METABOLISM

By Jigarkumar V. Desai, M.S.

A dissertation submitted in partial fulfillment of the requirements for the degree of Master's of Science at Virginia Commonwealth University.

Virginia Commonwealth University, 2010

Major Director: Dr. Martin K. Safo
Associate Professor, Department of Medicinal Chemistry

Pyridoxal kinase (PL kinase) and pyridoxine 5'-phosphate oxidase (PNP oxidase) are the two vitamin B_6 salvage enzymes involved in metabolism of the primary inactive vitamin B_6 (pyridoxal, pyridoxine and pyridoxamine) into the active cofactor form, pyridoxal 5'-phosphate (PLP). PLP, arguably the most important vitamin, is required by numerous vitamin B_6 (PLP-dependent) enzymes as a co-factor. These enzymes serve vital roles in the metabolism of glucose, lipids, amino acids, heme, DNA/RNA and many neurotransmitters.

High levels of vitamin B_6 are linked to neurotoxicity, due to the non-specific interactions of PLP with non-B_6 proteins. This problem is controlled, in part, by maintaining a low *in vivo* concentration of free PLP (~1 μM); raising the intriguing question of how the cell regulates, as well as, supplies sufficient PLP to meet the requirements of B_6 enzymes. Similar to PLP excess, PLP deficiency, due to mutations in

PL kinase and PNP oxidase or drug-induced inhibition of their activity, has been implicated in many pathological conditions.

The objective of this study is to elucidate the mechanisms underlying PLP regulation by PL kinase, and its subsequent transfer to dozens of PLP-dependent enzymes. A second objective is to gain valuable information into whether a missense mutation (S261F) in PL kinase could affect the enzyme activity and/or structure. A third objective is to understand how vitamin B_6 metabolism by PL kinase is disrupted by the neurotoxic compound, ginkgotoxin.

The mutant (hPL kinase S261F) was obtained using site-directed mutagenesis. It was then expressed, purified and analyzed by circular dichroism, fluorescence spectroscopy, enzyme kinetics and native-PAGE. Our results showed no considerable differences between wild-type enzyme and the mutant, suggesting the mutation to be non-pathogenic.

PLP was found to inhibit PL kinase by binding to the substrate PL site in the presence of substrate MgATP to form an abortive ternary complex (PL kinase-PLP-MgATP). The physiological significance of this ternary complex was also analyzed and it was found to be a source of PLP transfer to apo B_6 enzymes.

Enzyme kinetics, affinity chromatography and fluorescence polarization techniques were used to test our hypothesis that the reactive PLP is transferred from PL kinase to apo-B_6 enzymes via channeling. Channeling should provide an efficient and protected way for PLP transfer from the kinase or oxidase to apo-B_6 enzymes. Our results provide a strong support to the channeling mechanism.

Ginkgotoxin was found to be a competitive inhibitor of PL kinase with a K_i of 18 μM. X-ray crystallographic analysis of its binding mode to PL kinase confirmed its binding to the substrate PL site of the enzyme. A unique hydrophobic interaction between its lipophilic side chain 4'-OCH_3 and nearby Tyr127 and Val231, in addition to the conserved PL binding interactions, was found to be responsible for its higher affinity to the enzyme.

CHAPTER 1

GENERAL INTRODUCTION

1.1 **B_6 vitamers:** Vitamin B_6 is arguably the most important vitamin. It consists of three different 3-hydroxy-2-methyl-pyridine derivatives, including pyridoxal (PL), pyridoxine (PN), and pyridoxamine (PM) (Figure 1). Plants and prokaryotes synthesize these B_6 vitamers *de-novo* from small metabolites, but mammalian cells cannot carry out *de-novo* synthesis.[4, 9, 10] They are mainly dependent upon dietary intake of the vitamins. The non-phosphorylated B_6 vitamers are not biologically active and must be phosphorylated to attain activity (Figure 1). Among the phosphorylated derivatives, only pyridoxal 5'-phosphate (PLP), and to a lesser extent, pyridoxamine-5'phosphate (PMP) is biologically active.[4-7]

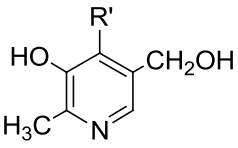

R' = CH_2OH; pyridoxine (PN)
R' = CH_2NH_2; pyridoxamine (PM)
R' = C(=O)H; pyridoxal (PL)

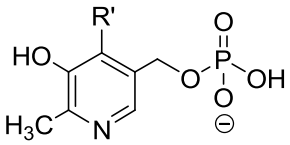

R' = CH_2OH; pyridoxine 5'-phosphate (PNP)
R' = CH_2NH_2; pyridoxamine 5'-phosphate(PMP)
R' = C(=O)H; pyridoxal 5'-phosphate (PLP)

Figure 1: **Structures of the B_6 vitamers**

1.2 Vitamin B_6 metabolism: The bio-activation of vitamin B_6 derivatives is carried out by two key enzymes; pyridoxal kinase (PL kinase) and pyridoxine 5'-phosphate oxidase (PNP oxidase). Together these enzymes are responsible for PLP synthesis in the salvage pathway, as shown in Figure 3. This pathway is active in both prokaryotes and eukaryotes, while *de-novo* pathway for PLP synthesis is only active in prokaryote, in which PLP is synthesized from erythrose-4-phosphate by a series of steps, as shown in Figure 2. In the salvage pathway

pyridoxal kinase carry out phosphorylation of all the three forms of vitamin B_6, by transferring γ-phosphate of ATP to 5'–OH group of B_6 vitamers; while PNP oxidase is responsible for oxidation of PNP and PMP to PLP in both the salvage and *de-novo* pathways (Figures 2 & 3). PLP is recycled during protein turnover via the salvage pathway involving PLP-phosphatase, PL kinase and PNP oxidase. Released PLP from proteins is first converted by the phosphatases to PL. PNP and PMP in the cells are also converted to PN and PM by phosphatases. These vitamers are then acted upon by the oxidase and kinase as described above. Pyridoxal 5'-phosphate (PLP) is required as a co-factor by over 140 different vitamin B_6 (PLP-dependent) enzymes to carry out their biological functions. These enzymes are involved in carrying out several diverse reactions including, but not limited to neuro-transmitter catabolism, synthesis of polyamines, methionine metabolism, heme biosynthesis, sphingomyelin synthesis, carbohydrate metabolism, nucleic acid synthesis and homocysteine metabolism.[1-3] The metabolism of B_6 vitamers can be illustrated schematically as shown in Figures 2 and 3;

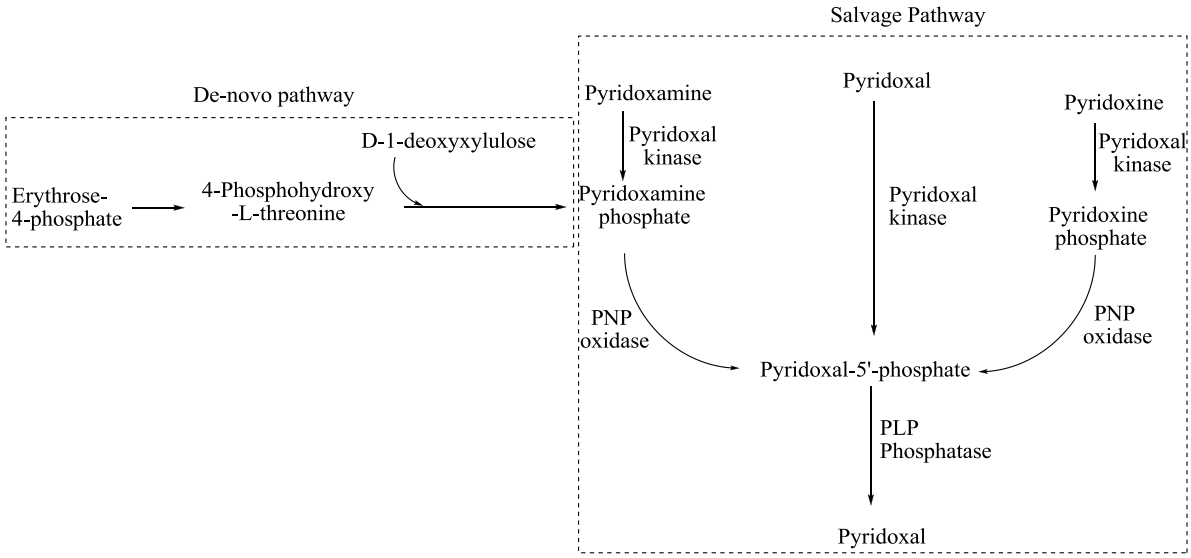

Figure 2: *De-novo* and Salvage pathways for PLP synthesis; *De-novo* being active only in prokaryotes, while Salvage pathway being active in both prokaryotes and eukaryotes

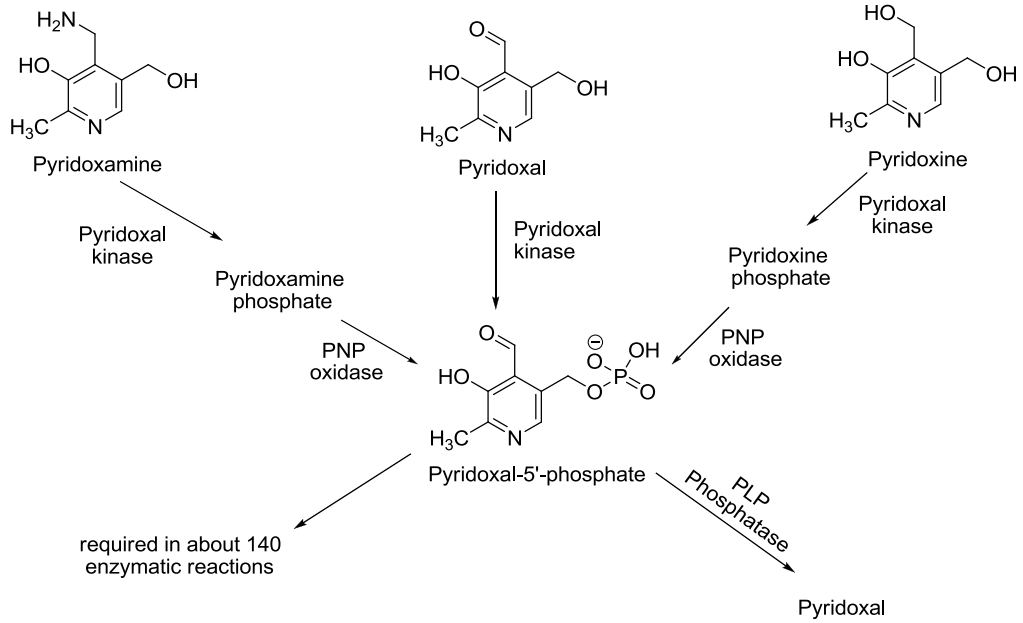

Figure 3: **Metabolism of B_6 vitamers (Salvage pathway)**

1.3 Pyridoxal kinase: This enzyme is responsible for phosphorylation of B_6 vitamers in the salvage pathway, in both eukaryotes and prokaryotes. It catalyzes the transfer of γ-phosphate from ATP to the 5'-CH_2OH of the B_6 vitamers, as shown in Figure 4. Most organisms possess PL kinase encoded by the gene *pdxK*, which is highly homologous among prokaryotes and eukaryotes.[5] In addition to the PL kinase coded by the *pdxK* gene, *E. coli* and several other prokaryotes are also found to contain a homolog PL kinase enzyme (PL kinase 2) coded by the gene *pdxY*. [4, 5, 9] PL kinase 2 shares very low sequence identity (~30%) with PL kinase.[5] This protein also functions in salvage pathway but is catalytically very less active as compared to PL kinase, therefore its exact role in vitamin B6 metabolism is not clear.[4]

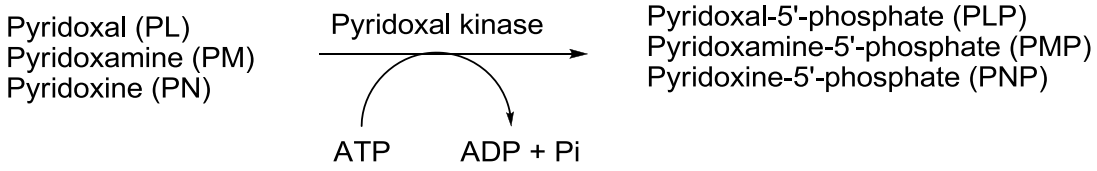

Figure 4: **Reaction catalyzed by Pyridoxal kinase**

The PL kinase enzyme follows random sequential addition of substrates.[6] There are several reports about the effects of monovalent and divalent metal cations on the activity of PL kinase and for optimal activity, K^+ and Mg^{2+} are required.[4, 6, 7, 9]

PL kinases have been purified from several organisms and for many of them crystal structures are also known.[5, 6, 9, 46] All of them show a typical ribokinase superfamily structure of core β-sheets surrounded by α-helices (Figure 5A).[6] All of them are dimers with active site in each subunit (Figure 5B), with conserved ATP and substrate binding geometries. Human enzyme

is more tolerant to changes in substrate chemistries, hence more prone to binding by substrate-like molecules, including many commonly used drugs.[6, 26]

A).

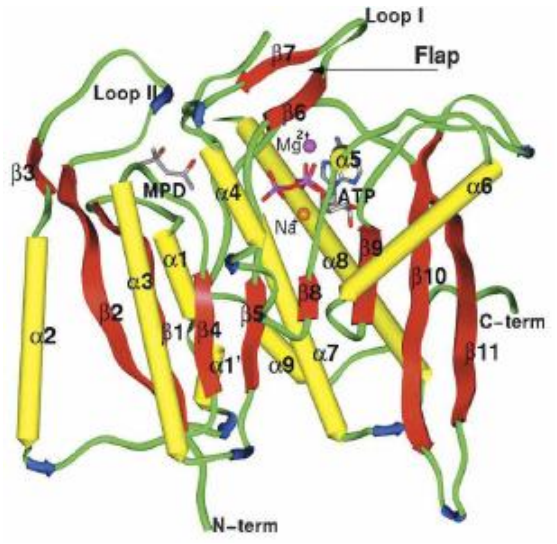

B).

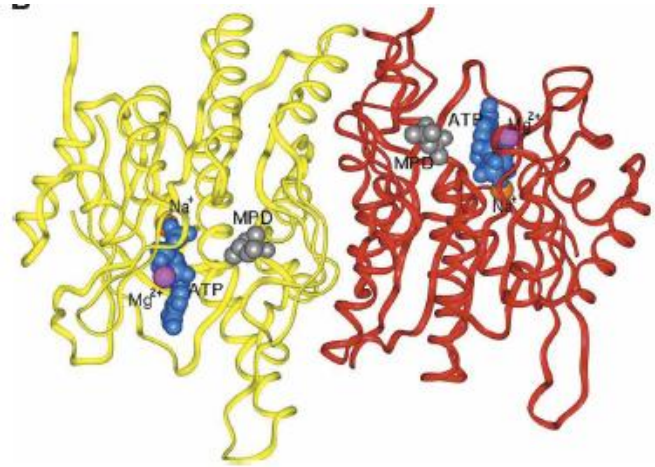

Figure 5: **Overall structure of hPL kinase.**[6] (A) The monomeric structure with bound ATP (stick), MPD (stick), Na^+ (brown sphere), and Mg^{2+} (magenta sphere) at the active site. α-Helices and β-strands are colored yellow and red, respectively. The secondary structures are labeled. (B) The dimeric structure, also with bound ATP (cyan CPK), MPD (gray CPK), Na^+ (brown sphere), and Mg^{2+} (magenta sphere). Monomers A and B are colored red and yellow, respectively.

1.4 Pyridoxine 5'-phosphate oxidase (PNP oxidase): PNP oxidase is a flavin mononucleotide (FMN) dependent enzyme, which catalyzes oxidation of PNP and PMP to PLP, as shown in Figure 6. It is a dimer having FMN bound to each subunit, which acts as an immediate electron acceptor, and is regenerated by transfer of the two electrons to oxygen forming hydrogen peroxide.[12] The activity of PNP oxidase is regulated by free PLP in cellular environment, since it acts as a product inhibitor of the enzyme activity.[35-38, 40, 41]

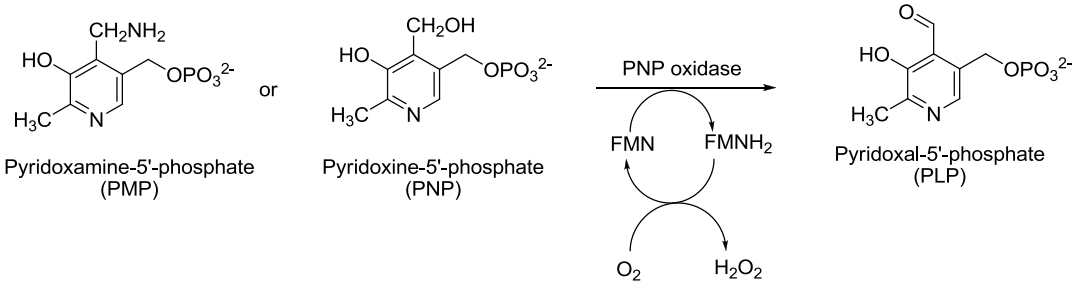

Pyridoxamine-5'-phosphate (PMP)

Pyridoxine-5'-phosphate (PNP)

Pyridoxal-5'-phosphate (PLP)

Figure 6: **Reaction catalyzed by PNP oxidase**

1.5 PLP dependent enzymes: The PLP, after being synthesized by PL kinase and/or PNP oxidase, is taken up by apo B_6 enzymes. It binds to a specific lysine residue through a Schiff base linkage, also called as an internal aldimine, and activates the apo enzyme to the holo form, as shown in Figure 7.[14] These PLP-dependent enzymes carry out diverse reactions such as racemization, decarboxylation, β and γ elimination and replacement reactions.[14, 16] Physiologically, these reactions are responsible for neurotransmitter synthesis, heme biosynthesis, one carbon unit transfer and hence nucleic acid biosynthesis, sphingomyelin synthesis and carbohydrate metabolism.[1]

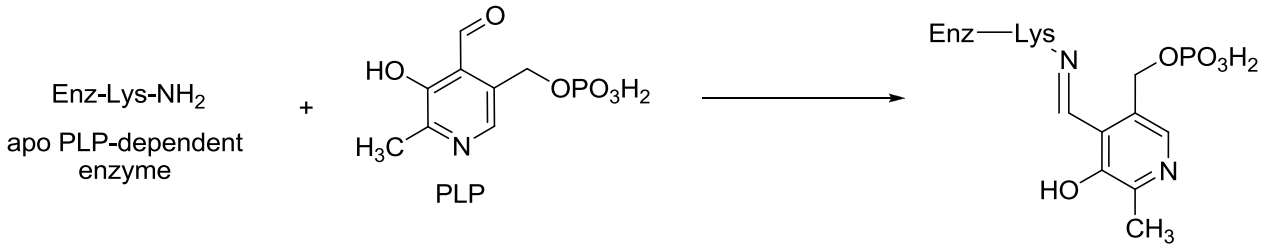

Figure 7: **Activation apo PLP-dependent enzymes to holo enzymes by binding of PLP to specific lysine residue at enzyme active site via a Schiff-base linkage**

Since the determination of the first structure of a PLP-dependent enzyme, aspartate aminotransferase (AAT), structures of several PLP-dependent enzymes have been determined and attempts have also been made to classify these enzymes. Table 1 shows one such classification in which the PLP-dependent enzymes were classified into five different subtypes according to the similarity in their fold; active site and amino acid sequence.[14-16]

Table 1: Classification PLP-dependent enzymes with representative examples of each class [15, 16]

Family	**Examples of PLP-dependent enzyme**
Fold type I	Aspartate amino transferase (AAT)
	Serine hydroxymethyltransferase (SHMT)
	Glutamate decarboxylase (GAD)
Fold type II	Serine dehydratase
	Cystathionine β-synthase
Fold type III	Ornithine decarboxylase
	Alanine racemase
Fold type IV	Branched-chain amino-acid amino transferase
Fold type V	Glycogen phosphorylase

The above classification aptly exemplifies diversity of the PLP-dependent enzymes. It also serves to explain the physiological significance of these enzymes, as well as of PLP, which is required as a cofactor for their activity. Any alteration in PLP level may adversely affect several body functions due to the malfunctioning of PLP-dependent enzymes.

1.6 Deficiency of PLP: Proper functioning of the PLP-dependent enzymes and thus optimal health are dependent upon optimal level of PLP. Pyridoxal 5'-phosphate deficiency has been implicated in several neurological and non-neurological disorders, such as induction and development of hormone-dependent breast and prostate cancers, convulsions, peripheral nervous system damage, impairment of immune response, epilepsy, and autism.[1, 62] Most dietary sources contain vitamin B_6, hence PLP deficiency due to dietary insufficiency is less prominent.[1] Major reasons for PLP deficiency can be attributed to malfunctioning of PL kinase and/or PNP oxidase, which may be caused either by pathogenic mutations or by drug induced inhibition of these enzymes' activity.

1.6.1 PLP deficiency due to pathogenic mutations: Several neurological and non-neurological disorders have been reported due to mutations in the genes coding for PL kinase and PNP oxidase.[17, 18, 19, 63, 64] These mutations may cause impairment of enzymatic activity, low protein expressions or disruption of regulation mechanisms which can ultimately lead to PLP deficiency.[19] Mutations in the gene coding for PNP oxidase have been implicated in neonatal epileptic encephalopathy (NEE). These mutations resulted in 70-82% reduction in enzymatic activity.[17, 19, 20, 64] Detailed characterization of one such pathogenic mutant (R229W) has been carried out in our lab and it was shown that the mutation resulted in decrease in cofactor (FMN), as well as substrate (PNP or PMP) binding to PNPO with concomitant decreased in enzymatic activity.[19] Similarly, defective PL kinase has been implicated in children suffering from autism.[19,

[64] Apart from these, the mutations have also been implicated in several other neurological disorders including Alzheimer's disease, Parkinson's disease, learning disabilities, attention deficit hyperactive disorder and anxiety disorders.[19] Although there is no direct evidence of linking each mutation to the disorder but detailed analysis of each mutation may serve in designing proper treatment for affected patient.

1.6.2 PLP deficiency due to drug induced inhibition of PL kinase activity: PL kinase inhibiting drugs can be classified into two main classes; first, direct inhibitors of the enzyme activity; second, molecules reacting with the B_6 vitamers and thereby inhibiting the enzymes.[21] First class includes commonly used drugs such as theophylline, enprofylline, roscovitine and lamotrigine, while the second class includes drugs such as isoniazid, levodopa, cycloserine and D-penicillamine.[21, 25] Many of the neuro-toxic effects of all the above mentioned drugs can be attributed to their inhibitory effects on PL kinase. For theophylline, it is well established that it inhibits PL kinase, to which it shows mixed inhibition.[22-24] The crystal structure of theophylline bound to pyridoxal kinase has been deposited to the PDB by our group. Roscovitine, a drug currently being tested as a potential anti-cancer agent, is relatively selective for its target (i.e. the cyclin dependent kinases), but recently it has been reported to bind to pyridoxal kinase at the pyridoxal binding site.[25] The crystal structure of roscovitine and its derivatives bound to pyridoxal kinase indicates the ability of the enzyme active site to accommodate molecules much larger than pyridoxal.[26] Recently, several groups pointed out that the toxic effects of ginkgotoxin can be attributed to its inhibitory effects on PLP-synthesizing enzymes. Ginkgotoxin is mainly obtained from the seeds and leaves of *Ginkgo biloba*. Various medications from *Ginkgo biloba* are widely used in the treatment of various conditions ranging from bronchial asthma, irritable bladder, depression, dizziness, tinnitus and several others.[27-31] These medications have prominent

presence in traditional Chinese, Japanese and European system of medicine. In Japan, the seeds, also called as "Gin-nan", are used as food and their consumption has resulted in about 70 food poisoning episodes since 1930.[28, 65] Apart from *G. biloba*, several *Albizzia* species also contain Ginkgotoxin which is responsible for a condition called "Albizziosis" (Ginkgotoxin poisoning) in S. African cattle and sheep.[66] The symptoms of the toxicity mainly include seizures, tonic/chronic convulsions, vomiting and impaired consciousness. The symptoms were found to be alleviated by administering PLP.[65] This indicates that the toxicity can be attributed to the inhibition of PL kinase or PNP oxidase, which leads to decrease in PLP levels. The molecular mechanism of PLP deficiency by Ginkgotoxin is still needed to be investigated.

For all the above mentioned drugs, adverse effects may be alleviated by co-administering vitamin B_6 supplements. Also, knowing the binding mode of these drugs with PL kinase may also help in selecting other putative molecules which may bind to PL kinase to elicit their adverse effect. These findings will be helpful in improving the pharmacological profiles of the corresponding drugs.

1.7 PLP toxicity: Excess levels of PLP have also been implicated in sensory and peripheral neuropathies.[67] Toxicity of PLP can be attributed to the electrophilic 4'-CHO group which can react with several cellular nucleophiles.[67] Because of this property, PLP is even used to label specific amino acids to study proteins.[31] Several toxicities have been reported due to reactivity of PLP. Excess use of vitamin B_6 has been implicated in sensory and peripheral neuropathies, parethesia, demyelination, and degeneration of sensory neurons in peripheral nerves.[67-70] PLP has been reported to bind $GABA_A$ receptors via Schiff base linkage. This binding precipitated tonic-clonic convulsions in mice.[32, 33] In a similar fashion, PLP was also found to inhibit the activity of phenol (aryl) sulfotransferase, a major detoxification enzyme.[34]

Thus, the cell requires tight regulation of PLP concentration to reduce its non-specific interactions and thus toxicity. Figure 8 summarizes how excess, as well as deficit levels of PLP are undesirable, necessitating tight regulation of cellular PLP levels.

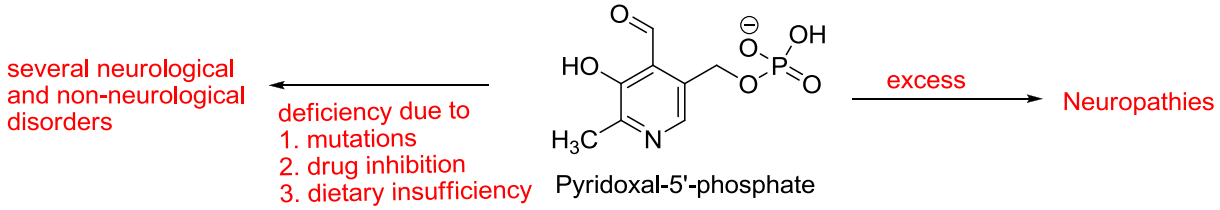

Figure 8: **Effects of PLP-deficiency and toxicity**

1.8 Regulation of PLP: Since excess levels of PLP in the cell is undesirable, free PLP levels have to be low. Several reports suggest that PLP does not accumulate in any body tissue.[35, 47] This raises the basic question of how the concentration of free PLP is regulated in body. Several regulatory mechanisms have been proposed and/or identified. These include action of PLP specific phosphatase, protein binding and feed-back inhibition of PNP oxidase. Among these, PLP specific phosphatase is believed to play very important role.[35, 39, 43] This enzyme is at least 10 fold more active than other phosphatase and it is much more specific for PLP.[39] This enzyme is homologous among all the species examined so far and it is found to be expressed ubiquitously in all the tissues with highest expression level in the brain.[39] This enzyme is responsible for dephosphorylation of PLP to the less reactive PL and it requires Mg^{2+} for its activity (Figure 9).[39, 67]

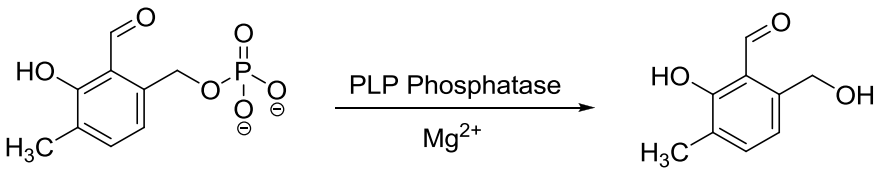

Figure 9: **Reaction catalyzed by PLP-phosphatase**

The k_{cat}/Km of 0.6 $\mu M^{-1}s^{-1}$ of this enzyme for PLP, as compared to 0.03 $\mu M^{-1}s^{-1}$ of PL kinase for PL, explains its high catalytic activity, as well as its importance in PLP homeostasis.[4, 39] In addition to the action of PLP-phosphatase, feed-back inhibition of PLP synthesizing enzymes is also believed to play a very important role in regulating PLP levels. Previously, it has been reported that PLP inhibits PNP oxidase at K_i of 1-25 μM.[35,44] Induced MgATP substrate inhibition of PL kinase in the presence of PLP has also been reported. Our group recently solved the crystal structure of PLP bound at the active site of PL kinase along with the substrate MgATP, as shown in Figure 10 – (Safo *et al.*, unpublished results). This suggests that PLP forms an abortive ternary complex with enzyme PL kinase and substrate MgATP. Binding of PLP at active site clearly indicates a possibility of competitive inhibition of enzyme activity by the product, PLP. The exact kinetic behavior of PLP inhibition for PL kinase is not known yet.

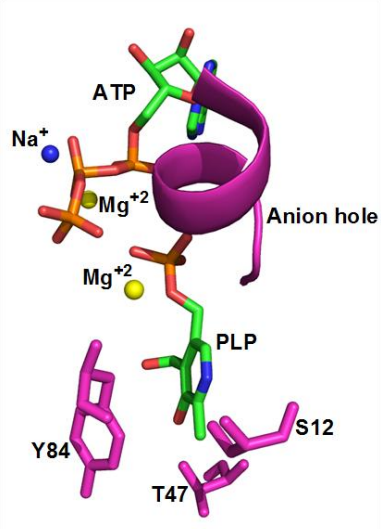

Figure 10: **Crystal Structure of Human PL kinase in complex with bound MgATP and PLP at the active site.**

1.9 Mechanism of PLP transfer: As mentioned in the preceding sections, PLP concentration is kept very low (~ 1μM) through several regulatory mechanisms, to reduce its toxicity.[35, 47] Despite this, over 140 apo B_6 enzymes manage to obtain enough PLP, which binds to a specific lysine residue at the active site of the enzymes and converts them to the fully functional holo form, as shown in Figure 7. The question is how they obtain PLP, despite its low *in vivo* concentration. Two possible mechanisms can be proposed, as shown in Figure 11.[35] According to mechanism I, synthesized PLP by PL kinase and/or PNP oxidase is first released as free PLP in the cytosol, which is then sequestered by apo B_6 enzymes. The released PLP is susceptible to dephosphorylation by PLP phosphatase to PL and may also react non-specifically with several other nucleophiles. The second mechanism (Mechanism II) is a channeling mechanism where PL kinase or PNP oxidase forms a complex with an apo B6 enzyme and transfers PLP, resulting in activation of apo B_6 enzyme to the holo form, without PLP on the kinase or oxidase being released into solvent. Substrate channeling has been previously reported for several different enzyme systems.[59, 71] It offers several distinct advantages such as; prevention of loss of intermediate by diffusion, protection of labile intermediates from solvent, and prevention of entry of intermediates to other metabolic pathways.[58,59] Previous studies have shown that PL kinase can interact with PLP-dependent enzymes like aspartate aminotransferase, glutamate decarboxylase, and alanine aminotransferase.[35, 47] A study by the Schirch group also showed that activation of apo B_6 enzyme to the holo form in cell extract was more efficient using PLP synthesized by PNP oxidase compared to the use of free PLP as shown in Figure 12.[12] The authors suggested that free PLP in the extract was forming non-productive aldimines with cell components, e.g. amino acids and proteins. These served to suggest a very strong possibility of PLP channeling.

Mechanism I:

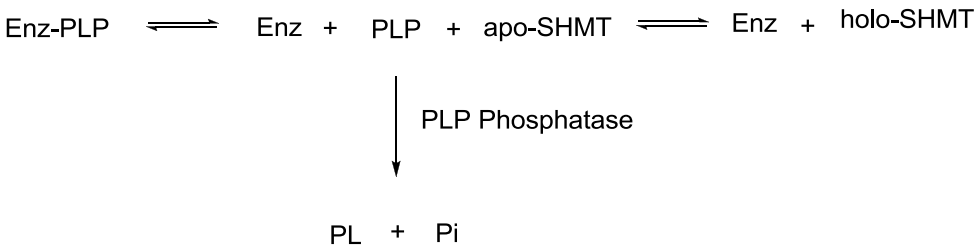

Mechanism II:

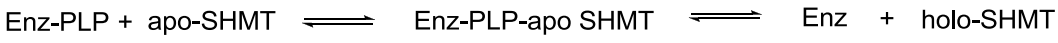

Figure 11: **Hypothetical mechanisms for transfer of PLP from PLP synthesizing enzymes to apo PLP-dependent enzymes**

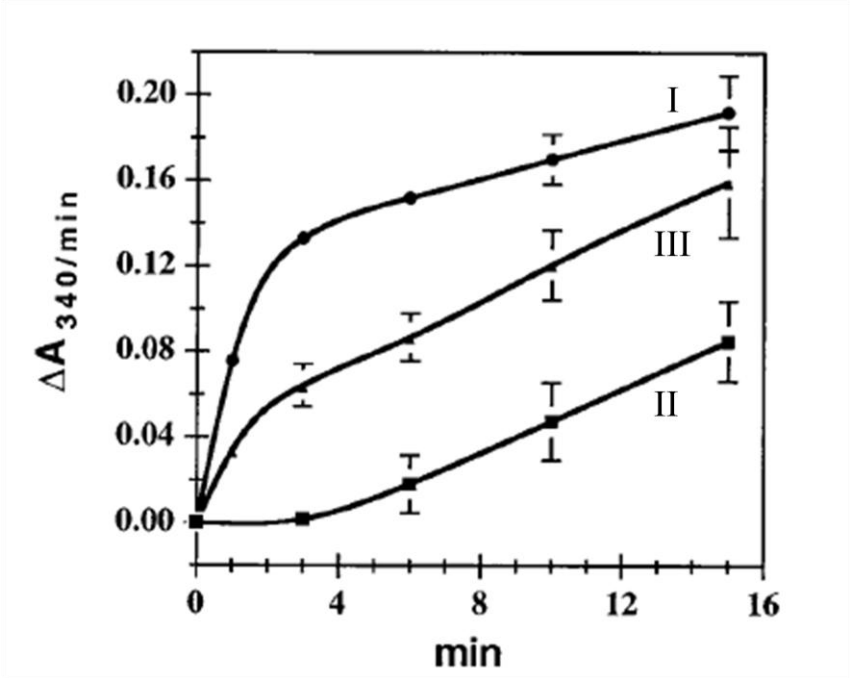

Figure 12: Activation of apo eSHMT by PLP and apo PNP oxidase-PLP[12]. (I) Apo eSHMT, 20 μM, was incubated with 25 μM PLP in 20 mM potassium phosphate, pH 7.3. Aliquots (5 ml) were removed every few minutes and assayed for eSHMT activity by observing the increase in absorbance at 340 nm/min in a coupled enzymatic assay. (II) Apo eSHMT was incubated under the same conditions as described above except the phosphate buffer included 0.3 g/ml of dried *E. coli* cell extract that lacks any SHMT activity. (III) Apo eSHMT, 20 mM, was incubated in the *E. coli* cell extract except the PLP was replaced with 25 μM PNPO-PLP

1.10 Rationale and Specific Aim

Vitamin B_6, as PLP, serves as a co-factor in over 140 enzymatic reactions and any decrease in PLP level in the cell, either due to mutations in the genes coding for PL kinase and/or PNP oxidase or drug induced inhibition of their activity, results in malfunctioning of PLP-dependent enzymes, which leads to several neurological, as well as, non-neurological disorders. The PLP levels, above physiological limit, have also been implicated in several neuropathies. Thus tight regulation of PLP concentration is required in the cell. The *overall objective* of this study is to elucidate the mechanisms underlying PLP metabolism and regulation, and its subsequent transfer to dozens of PLP-dependent enzymes. Another objective is to gain valuable information into how pathogenic mutations in PL kinase as well as inhibition of this enzyme by compounds disrupt vitamin B_6 metabolism. The study is divided into four specific aims;

1. Determine the kinetic regulation of PLP by PL kinase and the mechanism of PLP transfer to apo B_6 enzymes
2. Characterize protein-protein interactions between PL kinase and B_6 enzymes
3. Determine the effect of PL kinase S261F mutation on PL kinase activity and structure
4. Determine the effect of ginkgotoxin on PL kinase activity and structure

CHAPTER 2

DETERMINE THE KINETIC REGULATION OF PLP BY PL KINASE AND THE MECHANISM OF PLP TRANSFER TO APO B_6 ENZYMES

2.1 Introduction: The non-specific interactions of PLP with non B_6 proteins, due to high chemical reactivity of the aldehyde group on PLP, are controlled in part by maintaining a low *in vivo* concentration (~1 μM) by several regulatory mechanisms. These mechanisms include the action of PLP phosphatase and protein binding of PLP.[35, 39, 62, 81] Feed-back inhibition of PNP oxidase activity by PLP also plays an important role.[36-38] In addition, inhibition of human PL kinase activity by the product ADP (Safo *et. al.* - unpublished results), and the substrate MgATP in presence of PLP,[4] have also been reported. However, unlike the PNP oxidase, there are no detailed studies on the regulatory effect of PLP on PL kinase activity.

The low *in vivo* concentration of free PLP, as well as its highly reactive nature raises an intriguing question of how the cell supplies sufficient PLP, with high specificity, to the dozens of B_6 enzymes. There are two possible mechanisms for PLP transfer to apo B_6 enzymes-via channeling of PLP from the kinase or oxidase to the apo B_6 enzymes, or via release of the PLP from the kinase and oxidase into cytosol as free PLP which then finds its way to the apo B_6 enzymes.

This chapter focuses on elucidating the effects of PLP on catalytic activity of PL kinase, as well as determining the significance of a ternary abortive complex formed between PL kinase, MgATP and PLP (referred to as PL kinase-PLP-MgATP). We will also elucidate the mechanism involved in the transfer of PLP from PL kinase to activate apo B_6 enzyme to the holo form.

2.2 Materials: Bacterial culture media ingredients were purchased from Fischer Scientific (Pittsburgh, PA) and American Bioanalytical (Natick, MA). All the substrates were purchased from Sigma (St. Louis, MO) or Fischer Scientific (Pittsburgh, PA). Sephadex G50 was purchased from Fischer Scientific (Pittsburgh, PA). DEAE sephadex, ceramic hydroxylapatite, and CM sephadex were purchased from Sigma (St. Louis, MO). Nickel nitriloacetic acid (NiNTA) was purchased from Qiagen (Valencia, CA). Centrifugal filter devices were obtained from Milipore (Bedford, MA). The recombinant plasmid containing the gene insert coding for PLP-phosphatase was obtained from the Boe group (Bergen, Norway).

2.3 Methods

2.3.1 Expression and purification of human PL kinase (hPL kinase): The human PL kinase was purified using the procedure described previously.[5, 11] Briefly, competent *E. coli* Rosetta (DE3) pLysS cells (Novagen) were transformed with a pET28b vector carrying the human *pdxK* gene insert. Transformants were grown in 6 liters of LB-kanamycin-chlroamphenicol (kanamycin 50 μg/mL and chlroamphenicol 34 μg/mL) media and after reaching optical density of 0.8 at 600 nm, were induced with 0.5 M mM IPTG. Cells were grown for additional 5 hours at 32ºC and harvested by centrifugation. The cell pellets were re-suspended in 250 ml of 50 mM sodium phosphate buffer, pH 8.0 and rapidly ruptured by high pressure homogenization using *Avestin* cell disrupter. Streptomycin sulfate was added to a final concentration of 10 g/L to remove excess nucleic acids. After ammonium sulfate fractionation (at 30% and 60% saturation), enzyme was dialyzed in 50 mM sodium phosphate buffer, pH 8.0. The desalted protein solution was loaded on Ni-NTA column which was equilibrated with 50 mM monobasic sodium phosphate, pH 8.0, containing 300 mM NaCl, and 5 mM imidazole. The

column was washed thoroughly with equilibration buffer until OD_{280} was less than 0.1, and further washed several times with the same buffer, containing higher concentration of imidazole (10-75 mM). The enzyme was eluted from the column with 50 mM monobasic sodium phosphate buffer, pH 8.0, containing 300 mM NaCl, and 150 mM imidazole. Fractions containing 95% purity, as judged by SDS-PAGE, were pooled and the protein solution was concentrated by precipitation with 60% ammonium sulfate. The protein pellets were stored at -20°C for further usage.

2.3.2 Assay of PL kinase activity: The analysis of activity was carried out in 1cm thermostated cuvette in *Agilent 8454* spectrophotometer at 37°C by recording increase in $OD_{388\ nm}$, which indicates PLP formation from PL in presence of MgATP, as shown in Figure 13.[4] PL kinase (10-20 μM) was mixed with 1 mM MgATP in 20 mM sodium BES, pH 7 and the reaction was started by addition of 150 μM PL. The increase in OD at 388 nm was recorded for 60 seconds in kinetic mode of the software.

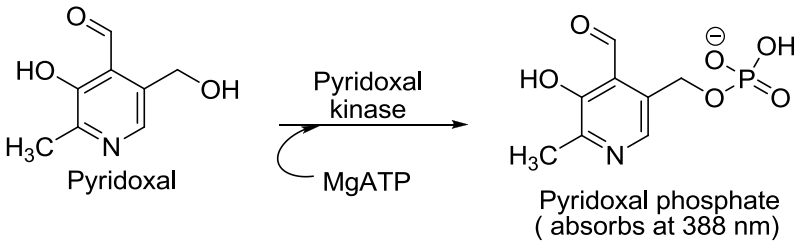

Figure 13: Assaying pyridoxal kinase activity

2.3.3 Expression and purification of *E. coli* serine hydroxymethyltransferase (eSHMT): The eSHMT was purified by a previously reported method, with minor modifications.[49] Briefly, the cDNA of gene *glyA*, coding for eSHMT, was inserted in vector pGS 29. The recombinant plasmid was transformed in *E. coli* K-12 cells. Transformants were grown

in 6 L LB-ampicillin (ampicillin 100 µg/mL) media containing 25 mM potassium phosphate (pH 7.4) and 0.4% glucose, at 37°C until they left the log phase of growth, as monitored by $OD_{600nm,}$ and harvested by centrifugation. The cells, after re-suspension, were lysed by homogenization at high pressure using *Avestin* cell disruptor. After ammonium sulfate fractionation (50% and 75%), protein pellet was dissolved in 20 mM potassium phosphate buffer, pH 7.2 and dialyzed extensively against the same buffer containing 0.1 mM PLP and 1mM EDTA. The desalted protein was loaded on DEAE-Sephadex column, which was pre-equilibrated with 20 mM potassium phosphate buffer, pH 7.2 The column was washed thoroughly with the equilibration buffer until OD at 280nm was below 0.2 and then the protein was eluted with linear salt gradient of 400 mL equilibration buffer and 400 mL of 50 mM potassium phosphate buffer, pH 6.4 containing 300 mM NaCl. Spectra of each fraction were recorded using UV-Visible spectrophotometer between 250-550nm. The fractions having value of OD_{280nm}/OD_{423nm} ratio below 50 were collected and analyzed by SDS-PAGE analysis for purity. Fractions containing pure protein were pooled together and protein was precipitated by adding ammonium sulfate to 75% saturation. The precipitate was dissolved in 20 mM sodium BES buffer, pH 7 and dialyzed against the same buffer containing 0.1 mM PLP. The activity of desalted protein was analyzed. It was then loaded on hydroxylapatite column, pre-equilibrated with 20 mM sodium BES, pH 7. The column was washed thoroughly with equilibration buffer until OD at 280nm was below 0.2 The protein was eluted with linear gradient of 50 mL equilibration buffer and 50 mL of 100mM potassium phosphate buffer, pH 7. The fractions having value of OD_{280nm}/OD_{423nm} ratio below 50 were collected and analyzed by SDS-PAGE analysis. Fractions of highest purity were pooled together. The pooled fractions were finally loaded on TMAE column, from which protein of almost 95% purity was obtained.

2.3.4 Expression and purification of rabbit cytosolic serine hydroxymethyltransferase (rcSHMT): The rcSHMT was expressed and purified by a previously reported method.[50] Briefly, the recombinant plasmid containing the gene insert coding for rcSHMT was transformed into *E. coli* HMS (DE3) cells. Transformants were grown in 6 L LB-ampicillin (ampicillin, 100 μg/mL) media containing 0.5% glucose, and buffered with 50 mM phosphate (pH 7.3), prepared from dibasic potassium phosphate and monobasic sodium phosphate. Cells were grown at 37°C till OD_{600nm} reached 1.2, induced with 0.5 mM IPTG, grown for additional 7 hours and then harvested by centrifugation. Cell pellets were re-suspended in 20 mM potassium phosphate, pH 7.3 containing 0.1 mM PLP, 5 mM 2-mercaptoethanol and 0.1 mM EDTA and ruptured by high pressure homogenization using *Avestin* cell disruptor. The protein was then precipitated by adding ammonium sulfate to 55% saturation. The precipitate was dissolved in 20 mM potassium phosphate buffer, pH 6.8 and dialyzed extensively against the same buffer containing 0.1 mM PLP and 1mM EDTA. This desalted protein was loaded on CM-Sephadex column, pre-equilibrated with 20 mM potassium phosphate buffer, pH 6.8. The column was washed thoroughly with the equilibration buffer until OD at 280nm was below 0.2 Protein was eluted with linear gradient containing 600 mL equilibration buffer and 600 mL of 300 mM potassium phosphate buffer, pH 7, containing 5 mM 2-mercaptoethanol and 0.1 mM EDTA. The spectra of fractions were recorded between 250-500 nm using UV-visible spectrophotometer. Fractions having OD_{280nm}/OD_{423nm} ratio less than 50 were collected and analyzed by SDS-PAGE. Fractions containing pure protein were pooled together and the protein was precipitated by adding ammonium sulfate to 60% saturation. The precipitate was dissolved in 20 mM potassium phosphate buffer, pH 7.3 containing 5 mM 2-

mercaptoethanol, 0.1 mM EDTA and 0.1 mM PLP. It was dialyzed against the same buffer and this desalted protein was analyzed for activity and stored at -20°C for further usage.

2.3.5 Activity analysis of Serine hydroxymethyltransferase: Activity analysis of SHMT was carried out by a coupled reactions assay.[49, 50, 56] In the assay, allothreonine was used as a substrate for SHMT and the rate of formation of acetaldehyde was measured by reducing it to ethanol by NADH and alcohol dehydrogenase. NADH absorbs at 340nm, but when it gets oxidized to NAD^+ during reduction of produced acetaldehyde to ethanol, gradual decrease in OD_{340nm} is observed. Therefore the activity of SHMT was monitored by recording change in OD_{340nm} in 1 cm thermostated cuvette at 30°C using *Agilent 8454* spectrophotometer. About 10 µg SHMT was mixed with 90 µg alcohol dehydrogenase and 180 µg NADH in 50 mM sodium BES buffer, pH 7.3 The reaction was started by addition of 10 µM allothreonine and decrease in OD at 340 nm was followed for 60 seconds.

2.3.6 Expression and purification of human PLP-phosphatase: The human PLP-phosphatase was purified by a previously reported procedure with minor modifications.[39] The recombinant plasmid containing the gene insert, coding for PLP-phosphatase, was transformed to *E. coli* HMS (DE3) pLys cells. The transformants were grown in 6 L LB-ampicillin media (ampicillin 100µg/mL). Cells were grown at 37°C until OD_{600nm} reached 0.6, induced with 50 µM β-isopropylthiogalactopyranoside (IPTG), grown for additional 24 hours at 18°C and then harvested by centrifugation. The cell pellets, after re-suspension, were lysed by high-pressure homogenization using *Avestin* cell disruptor. Streptomycin sulfate was added to the cell lysate at final concentration of 10g/L to remove excess nucleic acids. After centrifugation, the lysate was loaded on NiNTA column, pre-equilibrated with 50 mM monobasic sodium phosphate, pH 8.0, containing 300 mM NaCl, and 5 mM imidazole. The column was washed thoroughly with

equilibration buffer until the OD_{280} was less than 0.1, and further washed several times with the same buffer, containing higher concentration of imidazole (10-75 mM). The enzyme was eluted from the column with 50 mM monobasic sodium phosphate buffer, pH 8.0, containing 300 mM NaCl, and 150 mM imidazole. Fractions containing 95% purity, as judged by SDS-PAGE, were pooled and the protein solution was concentrated by precipitation with 60% ammonium sulfate. The precipitate was dissolved in 0 mM sodium BES buffer, pH 7 containing 4 mM $MgCl_2$ and dialyzed against the same buffer. It was stored at -20°C for further usage.

2.3.7 Activity analysis of PLP-phosphatase: The analysis of PLP-phosphatase activity was carried out in 1cm thermostated cuvette in *Agilent 8454* spectrophotometer at 37°C by recording a decrease in $OD_{388\ nm}$, which indicates dephosphorylation of PLP to PL, as shown in Figure 14.[39, 43] PLP-phosphatase was taken in 20 mM sodium BES buffer, pH 7 containing 4 mM $MgCl_2$. The reaction was started by addition of the substrate PLP at concentration of 100 µM and decrease in OD at 388 nm was recorded for 60 seconds.

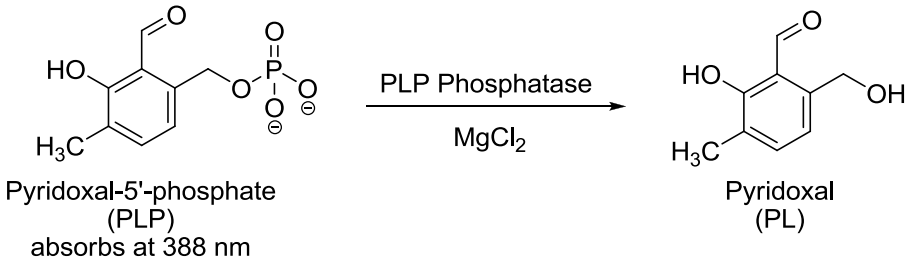

Figure 14: Assay of PLP-phosphatase activity

2.3.8 Preparation of ePL kinase-PLP-MgATP ternary abortive complex: PL kinase (300 µM) was mixed with its substrates, pyridoxal (PL, 400 µM) and MgATP (1 mM) in 20 mM sodium BES, pH 7 and incubated at 37°C for 1 hour. This reaction mixture was passed through Sephadex G50 column (0.6 x 45 cms), pre-equilibrated with 20 mM sodium BES, pH 7

containing 1 mM MgATP. About 400 µL fractions were collected and analyzed for eluted protein and PLP, by recording optical density at 280nm and 388nm respectively. Fractions containing high concentration of protein were pooled together and stored in 500 µL aliquots at -20°C for further use.

2.3.9 Preparation of apo serine hydroxymethyltransferase: Apo enzyme was prepared according to the method previously reported.[49] Briefly, holo SHMT (eSHMT or rcSHMT, 500 µL) was mixed with EDTA (1 µM), dithiothreitol (DTT, 1 µM), D-alanine (200 µM) and ammonium sulfate (200 µM) in 50 mM potassium phosphate buffer, pH 7. The reaction mixture was incubated at 37°C with shaking at 150-180 rpm until the yellow color disappeared. It was dialyzed extensively against 50 mM potassium phosphate, pH 7.4 containing 0.5 mM EDTA and 1mM DTT. The apo enzyme was quantified by measuring protein absorbance at 280 nm. It was then stored in 500 µL aliquots, containing 10% glycerol, at -70°C.

2.3.10 Determination of stoichiometry of PLP binding to ePL kinase-PLP-MgATP complex: The stoichiometry of PLP binding was analyzed by two different methods. In the first method, ePL kinase-PLP-MgATP (100 µL, 10-15 µM) was diluted to 900 µL and OD_{280nm} was measured to quantify protein. To this, NaOH solution was added to a final concentration of 0.1 N and OD_{388nm} was recorded. The released PLP was quantified using molar extinction co-efficient of 6600 $M^{-1}cm^{-1}$. In the second method, PLP was used to activate apo SHMT to holo SHMT. This holo SHMT ultimately forms a ternary quinonoid complex with glycine and tetrahydrofolate (THF) having absorption maximum at $OD_{491nm.}$ First, known concentrations of PLP (5-25 µM) were added to the reaction mixture of apo SHMT (20 µM), glycine (50 mM) and THF (100 µM). Formation of the quinonoid complex was followed for 15 minutes and ΔOD_{491nm}/15min values obtained for different concentrations of added PLP were used to plot a

standard curve of ΔOD_{491nm} versus PLP concentration. From the ePL kinase-PLP-MgATP complex, PLP was first released by adding it to 0.1 N NaOH solution. The complex was added to a final concentration of 10-15 μM. This mixture was then added to 350 μL of 100 mM sodium BES buffer, pH 6.5 to bring pH at 6.5. To this mixture; apo SHMT, glycine and THF were added to final concentrations of 20 μM, 50 mM and 100 μM respectively. The reaction was followed for 15 minutes and the ΔOD_{491nm}/15min value was recorded, which was further used to extrapolate the amount of PLP released from the standard curve. This amount of PLP was compared with the protein concentration to find out the stoichiometry of PLP binding.

2.3.11 Kinetic analysis of inhibition of PLP on PL kinase activity: The assay for PL kinase activity was carried out in 20 mM sodium BES buffer, pH 7 containing 2 mM $MgCl_2$ at 37°C using *Agilent 8454* spectrophotometer as described previously under section 2.3.2. Substrates PL and MgATP were used at concentrations of 150 μM and 1 mM respectively, while PL kinase was used at concentration of 10 μM. Concentration of PLP was varied between 1-500 μM to analyze its effects on PL kinase activity. Initial velocity data were recorded and "% enzyme activity" was calculated. It was plotted against PLP concentration and fitted in *Sigmaplot-11*. An approximate K_i value for PLP inhibition was determined by using *Cheng-Prusoff equation*[42] (Equation 1), in which PL was considered as a substrate to which PLP acted as a competitive inhibitor.

$$K_i \cong \frac{IC_{50}}{1 + \frac{[S]}{K_m}} \ldots\ldots\ldots (1)$$

where, *[S]* = concentration of PL, 150 μM

K_m = 30 μM for PL

2.3.12 Test of compartmentation or channeling of PLP from ePL kinase to apo SHMT: The transfer of PLP from PL kinase to apo SHMT was followed by a coupled assay, in which the PLP synthesized by PL kinase was used to convert apo SHMT to holo form. This holo SHMT formed a ternary quinonoid complex absorbing at 491 nm. The enzymes ePL kinase (20 μM), apo eSHMT (20 μM) and PLP-phosphatase (3 μM) were mixed together with glycine (50 mM), tetrahydrofolate (100 μM) and MgATP (1 mM) in 20 mM sodium BES buffer pH 7. The reaction was started by addition of PL (20 μM) and increase in OD_{491nm} was followed for 15 minutes.

Controls were run in parallel. First control contained apo SHMT and PL kinase with all the substrates, but PLP-phosphatase was omitted. Second control contained free PLP, and apo SHMT with its substrates, but PL kinase and its substrates MgATP and PL were omitted. In this case, the reaction was started by addition of PLP to the enzyme mixture. Third control contained free PLP and apo SHMT with its substrates, but PL kinase, its substrates and PLP-phosphatase were omitted.

Similar experiments were run to analyze the transfer of tightly bound PLP from ePL kinase-PLP-MgATP to apo SHMT. For this, the enzymes apo SHMT (20 μM) and PLP-phosphatase (3 μM) were mixed with glycine (50 mM) and tetrahydrofolate (100 μM) in 20 mM sodium BES buffer, pH 7 containing 1 mM MgATP. Reaction was started by addition of tightly bound PLP (20 μM) in form of ePL kinase-PLP-MgATP complex and OD_{491nm} was followed for 15 minutes. Activation of apo SHMT by free PLP, in presence and in absence of PLP-phosphatase, was also followed as control. In another control, activation of apo SHMT was followed by addition of tightly bound PLP in form of ePL kinase-PLP-MgATP without the addition of PLP-phosphatase.

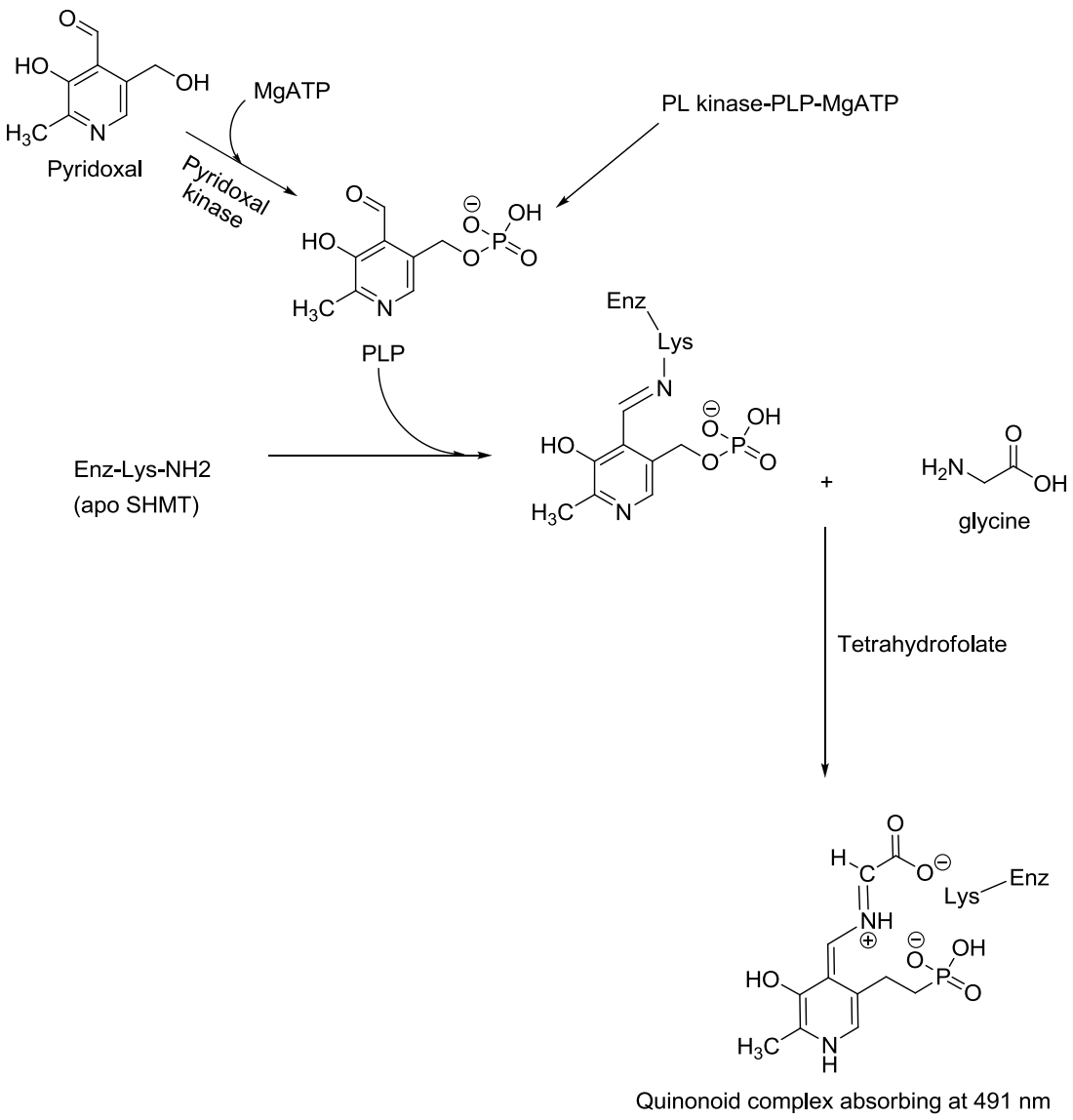

Figure 15: Scheme for following transfer of PLP from PL kinase to apo SHMT

2.4 Results and Discussion:

2.4.1 Purity of the enzymes: All the enzymes were >90% pure as judged by SDS-PAGE analysis. Figure 16 shows the pictures of gels after the final column in the purification of each enzyme;

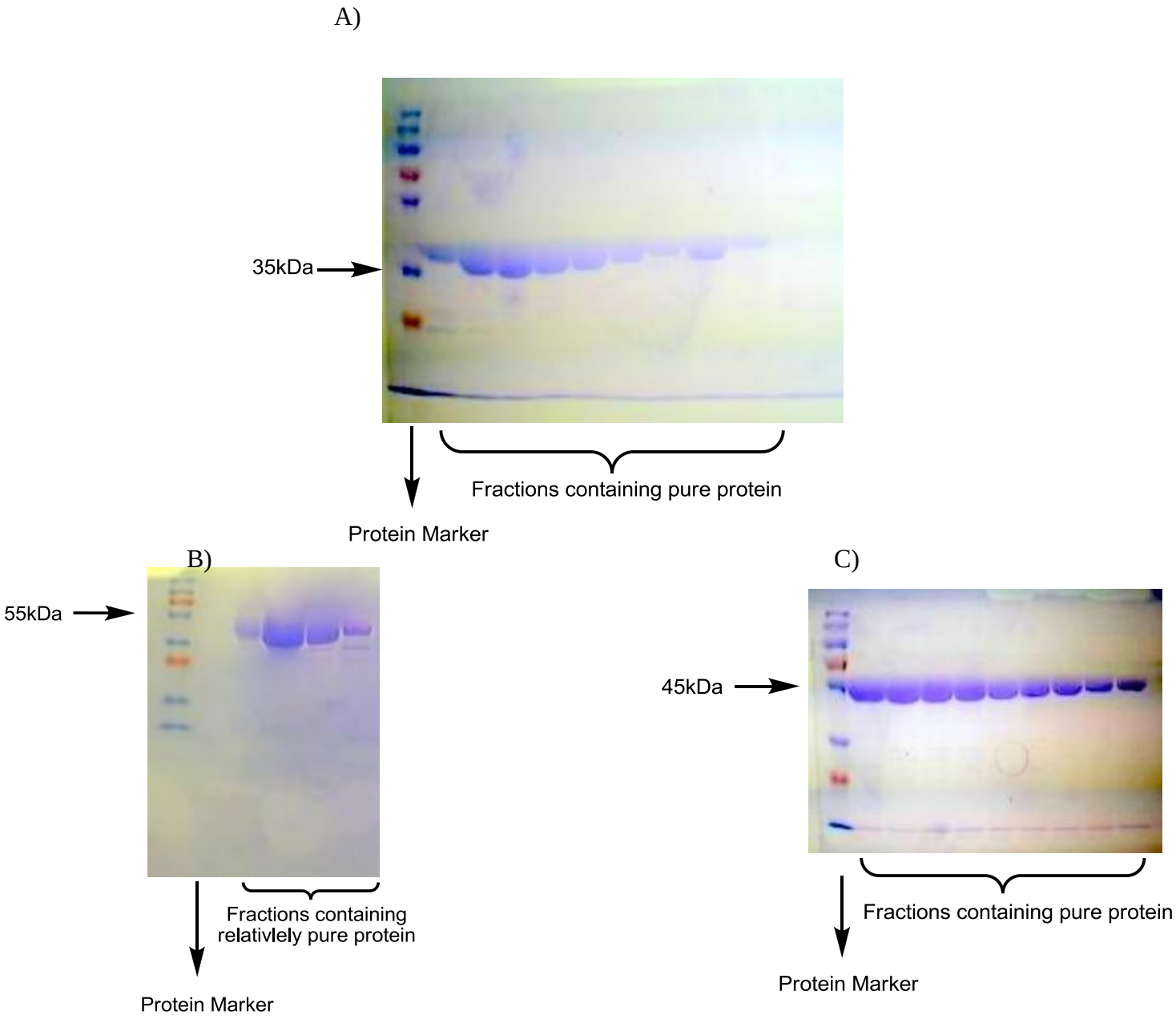

Figure 16: SDS-PAGE analysis of the fractions eluted out from the final column for purification of A) hPL kinase, B) eSHMT C) rcSHMT

2.4.2 Binding of PLP to PL kinase as a ternary complex with substrate MgATP (PL kinase-PLP-MgATP): PNP oxidase purified from brain and liver tissues was found to be inhibited by the product PLP at K_i ranging from 1-25 μM.[37, 38, 41, 44] Choi and Churchich reported that PLP in 10-fold excess inhibits sheep brain PNP oxidase significantly, and the inhibition was due to binding of PLP via aldimine linkage to a specific lysyl residue on protein.[36] Similarly, *E. coli* PNP oxidase was also found to be inhibited by PLP.[40] The characterization of PLP binding to *E. coli* PNP oxidase has also been carried out and PLP was found to bind tightly at a non-catalytic site of the enzyme.[12] This tightly bound PLP was found to be a very good source to activate apo SHMT in the cell extract, as compared to free PLP.[12] These observations suggest that PLP, in addition to exerting product inhibition on PNP oxidase, may bind to the enzyme at non-catalytic site, which may serve as a control mechanism for PLP regulation. PLP binding to human PL kinase has also been reported and the crystal structure of human PL kinase complexed to PLP and MgATP has been deposited to Protein Data Bank [PDB id 3KEU]. This crystal structure of PL kinase-PLP-MgATP shows PLP to bind at the active site of the enzyme at the PL site. In PL kinase structures, the 5'-OH group of the substrate PL is situated 6-7 Å away from the γ-phosphate of ATP, which provides room for co-existence of the 5'-phosphate of the product PLP and the substrate ATP together. The bound PLP remains anchored to the active site with the help of numerous interactions with amino acid side-chains and an additional Mg^{2+}, as shown in Figure 10. The crystal structure of PL kinase-PLP-MgATP gave an important insight into the binding mode of PLP. We have conducted studies to further characterize this ternary complex and also elucidate its possible inhibitory effect on PL kinase activity. The ePL kinase-PLP-MgATP complex was prepared by incubating the enzyme ePL kinase with substrates PL and

MgATP for an hour. The reaction mixture was then loaded on Sephadex G50 column. The elution profile is shown in Figure 17.

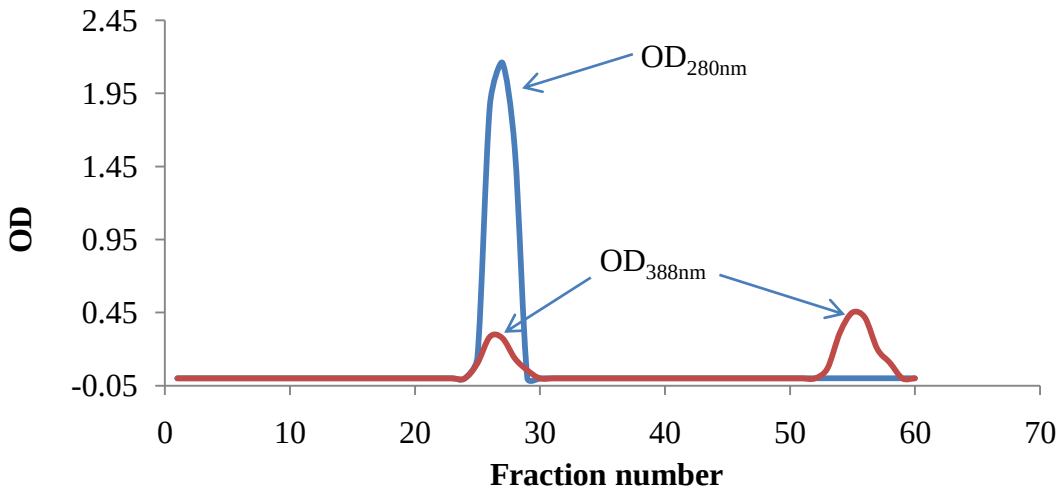

Figure 17: Elution profile of ePL kinase incubated with PL and MgATP after passing through Sephadex G50 (0.6 x 45 cms).

The elution profile shows peaks of protein (280 nm) and PLP (388 nm). The coincident rise of 388nm peak along with the protein peak clearly indicates the binding of PLP to PL kinase which absorbs at 388 nm. Apart from this, free PLP was separated effectively as seen from the elution profile. Most interestingly, and also observed previously for the tightly bound PLP on PNP oxidase, the bound PLP on PL kinase could not be separated from the protein by dialysis or even after passing it second time through the same column. This indicates the fact that PLP remains tightly bound to PL kinase.

2.4.3 Determination of stoichiometry of PLP binding: The stoichiometric binding of PLP to PL kinase was analyzed by two different methods. In each of these methods, bound PLP was first released by adding 0.1 N NaOH, which served to denature the protein and thus the release of bound PLP. In the first method, the amount of PLP released was determined by recording OD_{388nm} and using molar absorption co-efficient of 6600 $M^{-1}cm^{-1}$ for PLP.[12] Figure 18A shows the spectra of PLP, before and after the addition of 0.1N NaOH. In the second method, the released PLP, after neutralizing the solution, was used to activate apo SHMT which subsequently formed ternary quinonoid complex with glycine and tetrahydrofolate (THF), absorbing strongly at 491nm. It has molar extinction co-efficient of 20000 $M^{-1}cm^{-1}$. [12, 52, 53]A standard curve for formation of the quinonoid complex was plotted against the concentration of PLP used. The PLP released from ePL kinase-PLP-MgATP was quantified from this standard plot and compared to the protein concentration to determine the stoichiometry. Figure 18B shows the standard plot of ΔOD_{491nm} versus different PLP concentrations, from which PLP released from PL kinase-PLP-MgATP complex was quantified. Table 2 summarizes the results obtained by both methods and it indicates that one molecule of PLP binds to each subunit of PL kinase in 1:1 fashion.

A).

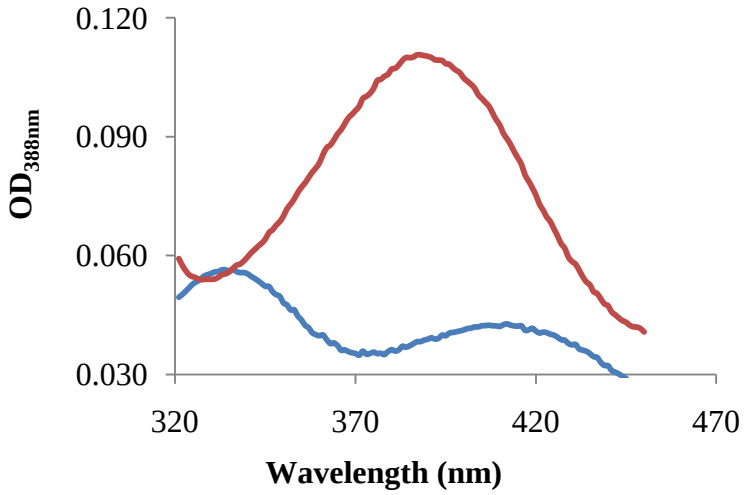

B).

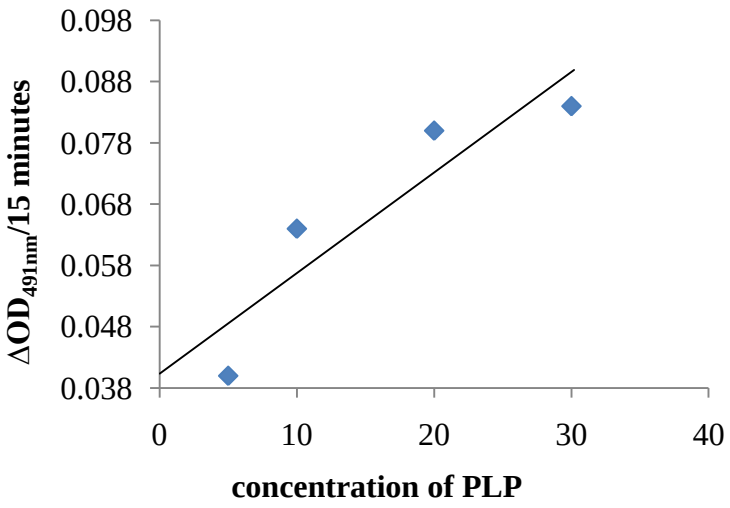

Figure 18: Determination of stoichiometry of PLP binding to ePL kinase-PLP-MgATP ternary abortive complex; A) Stoichiometry determination by OD_{388nm} method; blue curve shows spectra of the complex before addition of 0.1 N NaOH, while red curve is spectra of the complex after adding 0.1N NaOH, B) Stoichiometry determination using OD_{491nm} method

Table 2: Determination of stoichiometry of PLP binding to ePL kinase-PLP-MgATP complex

	OD_{388nm} method	**OD_{491nm} method**
Stoichiometry (Protein:PLP)	1.01	1.07

2.4.4 Inhibition of PL kinase activity by product PLP: The effect of PLP on the catalytic activity of PL kinase was analyzed spectrophotometrically. Figure 19 shows the profile for PLP inhibition of PL kinase activity. The IC_{50} and K_i for this inhibition by PLP are indicated in Table 3

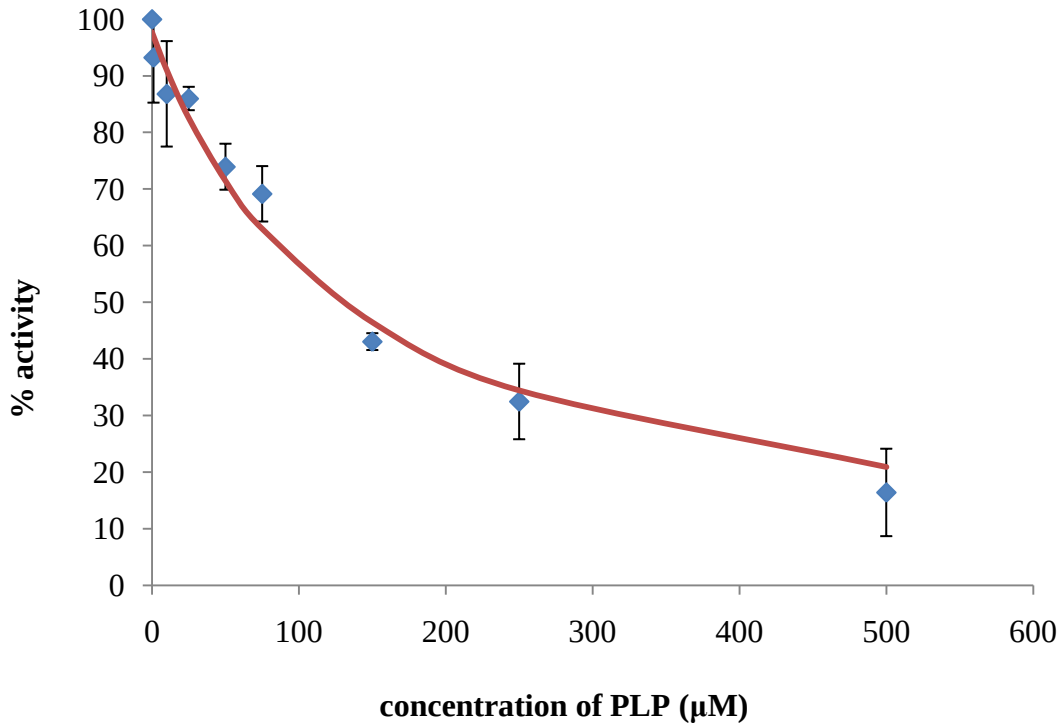

Figure 19: Inhibition of catalytic activity of PL kinase by product PLP; 10 µM PL kinase was checked for activity by converting 150 µM of PL to PLP by the transfer of γ-phosphate from MgATP (1 mM) in presence of PLP (1-500 µM)

Table 3: Kinetic parameters for inhibition of PL kinase activity by PLP

IC_{50}	135.9 ± 0.6 µM
K_i	22.7 ± 0.1 µM

The obtained K_i for PLP inhibition of PL kinase activity is comparable to K_i of 23 μM for PNP oxidase inhibition, reported by Churchich *et. al.*[44] This suggests that PLP may also be serving as a control factor in PL kinase activity, which acts in concert with other regulatory mechanisms to prevent the accumulation of highly reactive PLP in cellular environment.

The obtained K_i is still higher than the average concentration of free PLP found in cellular environment, but an explanation can be given for this. There are several reports of formation of protein-protein complexes between PL kinase and PNP oxidase, as well as, the complexes between PL kinase and other PLP-dependent enzymes like aspartate aminotransferase, alanine aminotransferase and glutamate decarboxylase.[35, 44, 47] This can be generalized for all the other PLP-dependent enzymes also, as described in following chapters. The formation of protein aggregates like these prevent the diffusion of PLP, which increases the local concentration of PLP to several-fold as compared to the cellular PLP levels. Keeping these facts in mind, it can be proposed that physiologically, PLP may self-regulate its intra-cellular levels by inhibition of the salvage enzymes, PL kinase and PNP oxidase.

2.4.5 Transfer of PLP from PL kinase to apo SHMT: We studied activation of apo B_6 enzyme using PLP produced during steady state catalytic activity of PL kinase from the substrates PL and MgATP. In a previous study Churchich *et al.*[35] showed that PL kinase and AAT interacted together prior to PLP transfer. They checked the possibility of PLP channeling by including a trapping agent (alkaline phosphates), and the results showed that the phosphatase did not have any effect on the rate of transfer, suggesting a possibility of channeling. Alkaline phosphatase, used in their studies, is relatively non-specific and has broad substrate specificity.[39] We conducted similar experiments with apo SHMT, and also used PLP-phosphatase instead of alkaline phosphatase as a trapping agent.

We analyzed the transfer of PLP by mixing ePL kinase, apo eSHMT and PLP-phosphatase together with MgATP, glycine and THF. The assay scheme is shown in Figure 15. The reaction was started by adding PL, which was converted to PLP by PL kinase and then incorporated into apo eSHMT to activate it. Control in the absence of PLP-phosphatase was also run. Another control using free PLP in the presence and absence of PLP-phosphatase were also conducted. Figure 20 shows the result of this experiment;

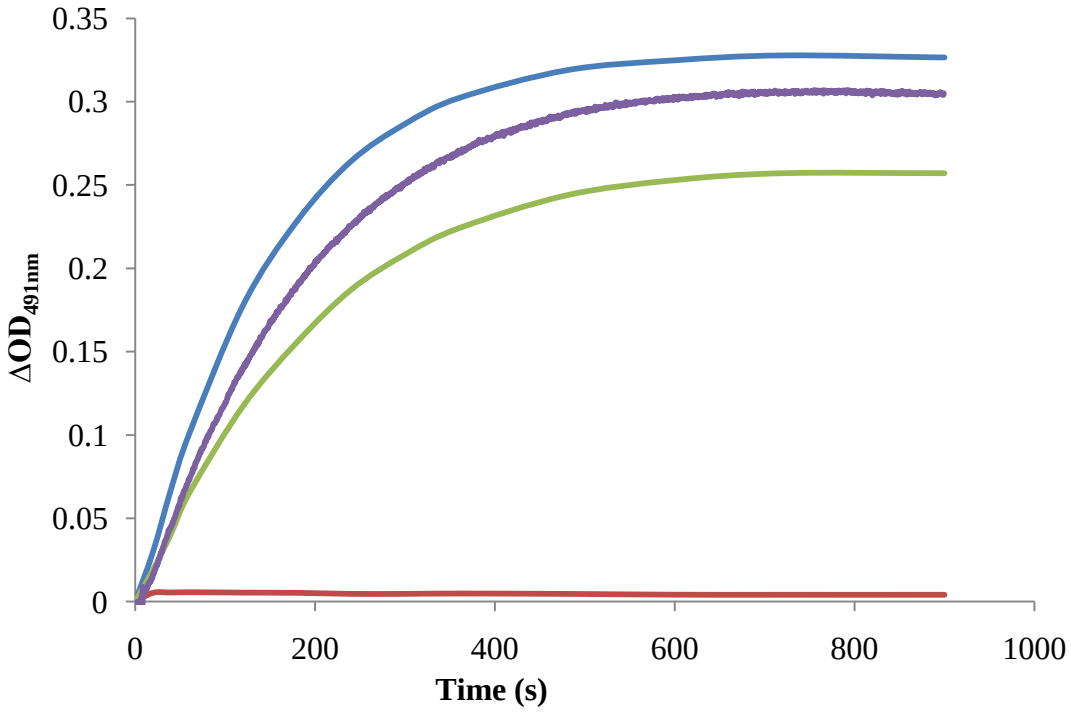

Figure 20: Test of compartmentation or channeling of PLP from ePL kinase to apo eSHMT; activation of apo SHMT by free PLP in absence (blue curve), and in presence of PLP-phosphatase (red curve). Activation of apo SHMT by PLP produced during steady state catalytic activity of ePL Kinase, in absence (purple curve), and in presence of PLP-phosphatase (Green curve)

From Figure 20, it is evident that PLP, after being synthesized by ePL kinase was efficiently transferred to apo eSHMT despite the presence of PLP-phosphatase (green curve), although there seems to be some slight effect by the phosphatase. Nevertheless, when free PLP was used to activate apo eSHMT, no activation was observed (red curve). In absence of PLP-phosphatase, activation either by free PLP (blue curve) or by PLP synthesized by ePL kinase in the reaction mixture is almost similar (purple curve). This trapping experiment, although does not conclusively prove channeling, but definitely proves that free PLP was not involved in the transfer. For channeling to occur; both proteins, ePL kinase and eSHMT, should associate to form a protein-protein complex. The study to characterize this complex formation is discussed in chapter 3.

2.4.6 Transfer of tightly bound PLP on ePL kinase (ePL kinase-PLP-MgATP complex) to apo SHMT: We have shown above that PLP binds tightly at the active-site of PL kinase. The PLP remains bound even after dialysis or even passing it through the sizing column. To determine if the tightly bound PLP can be transferred to apo B_6 enzyme and the mode of transfer, we followed the activation of both *E. coli* and rabbit apo SHMT with *E. coli* PL kinase-PLP-MgATP complex in the presence and absence of PLP-phosphatase. Controls were run by following activation of apo eSHMT and rcSHMT with free PLP, in absence and presence of PLP-phosphatase. Figures 21 and 22 shows the result of the experiment;

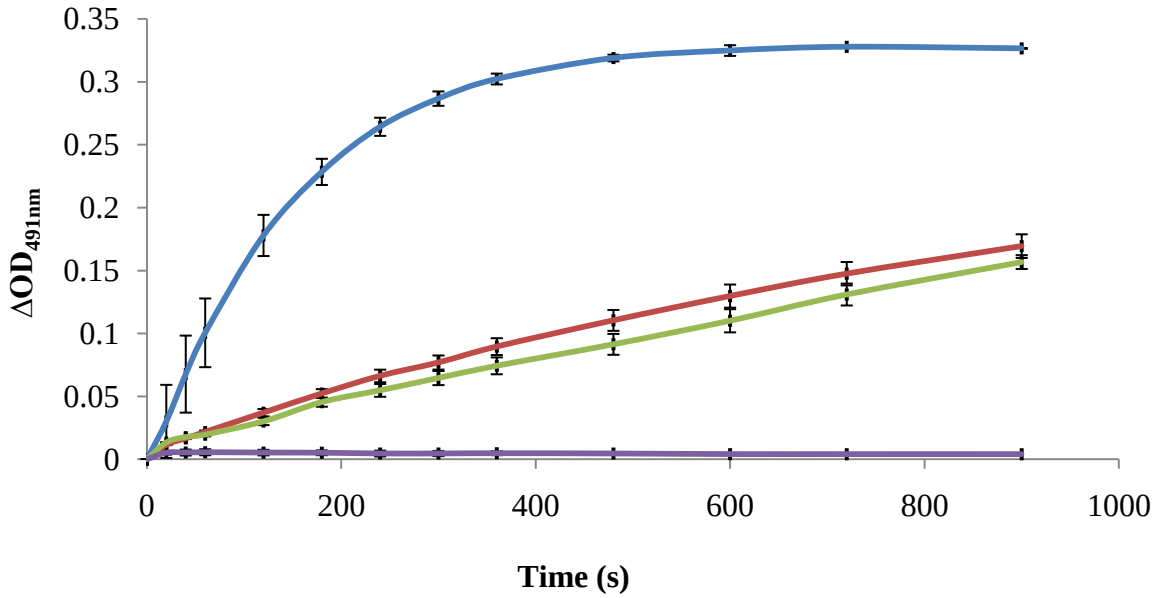

Figure 21: Activation of apo eSHMT by PLP (free and tightly bound); activation of apo eSHMT by free PLP, in absence (blue curve) and in presence of PLP-phosphatase (purple curve). Activation of apo enzyme by tightly bound PLP on ePL kinase-PLP-MgATP complex in presence (red line) and in absence of PLP-phosphatase (green curve)

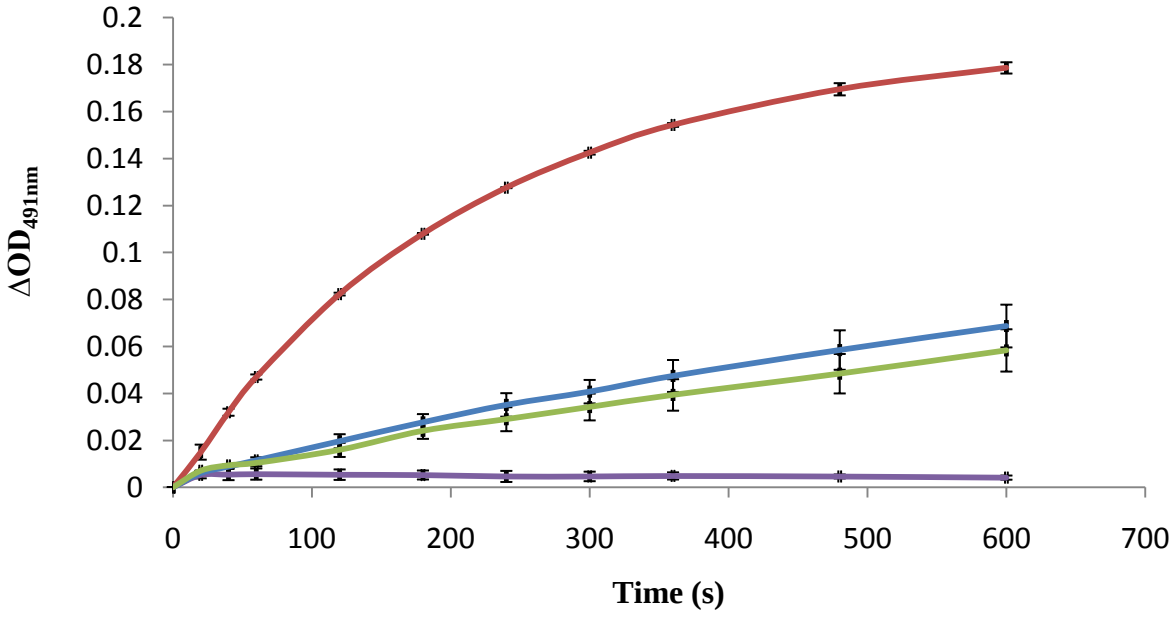

Figure 22: Activation of apo rcSHMT by PLP (free and tightly bound); Activation of apo rcSHMT by tightly bound PLP from ePL kinase-PLP-MgATP in absence (blue curve) and in presence of PLP- phosphatase (green curve). Activation of apo rcSHMT by free PLP in absence (red curve) and in presence of PLP- phosphatase (purple curve)

The results, as shown in Figure 21, suggest that the tightly bound PLP, which did not separate from ePL kinase-PLP-MgATP complex by dialysis and passage through sizing column, was easily transferred to apo eSHMT to activate the enzyme (red curve). This transfer was found to be almost not affected by action of PLP-phosphatase (green curve), while free PLP was completely inhibited from activating the apo B_6 enzyme in the presence of the phosphates (purple curve). We observed similar results when rabbit cytosolic serine hydroxymethyltransferase (rcSHMT) was used instead of eSHMT (Figure 22). This study shows that the ternary complex may be a source of PLP for activation of apo B_6 enzyme, and also the result gives additional support to the channeling mechanism. The results were also consistent with the observation by Yang and Schirch[12] that PNP oxidase-PLP is a better source of PLP for apo SHMT activation as compared to free PLP in cell extract.

Although the concentrations of free PLP and PLP on PL kinase-PLP-MgATP are the same, the rate of activation by free PLP is about twice that of the complex. This is in contrast to the transfer study using steady state production of PLP. At present we do not have any explanation, but it could be that PL kinase-PLP-MgATP forms a non-dissociating complex with B_6 enzymes and, which may hinder PLP channeling to all available sites on B_6 enzymes. In effect there is only a half-site transfer. Consistently, if free PLP is added to this complex after 700 sec (see Fig. 21 & 22), we observe fully activated SHMT.

2.4.7 Transfer of tightly bound PLP on ePL kinase (ePL kinase-PLP-MgATP complex) to apo SHMT in absence of MgATP: We have shown that MgATP is important in forming the ternary PL kinase-PLP-MgATP complex. The X-ray structure shows intimate interaction between the phosphate of the ATP and phosphate of the PLP mediated by Mg^{2+} ion. The above transfer study with ePL kinase-PLP-MgATP involves the use of additional MgATP (1

mM) in the reaction buffer to keep the enzyme in the abortive form. To test whether we will observe similar apo B_6 activation profile without extra MgATP, we repeated the above experiment without extra MgATP. The result is shown in Figure 23, and it indicates that in the presence of PLP-phosphatase the activation of apo eSHMT was found to be lower (green curve), as compared to the control in which PLP-phosphatase was omitted (red curve). This is in contrast to the previous experiment with extra MgATP that showed presence and absence of phosphatase resulted in similar activation. This suggests the importance of Mg^{2+} in stabilizing the binding of both ATP and PLP at the active site.

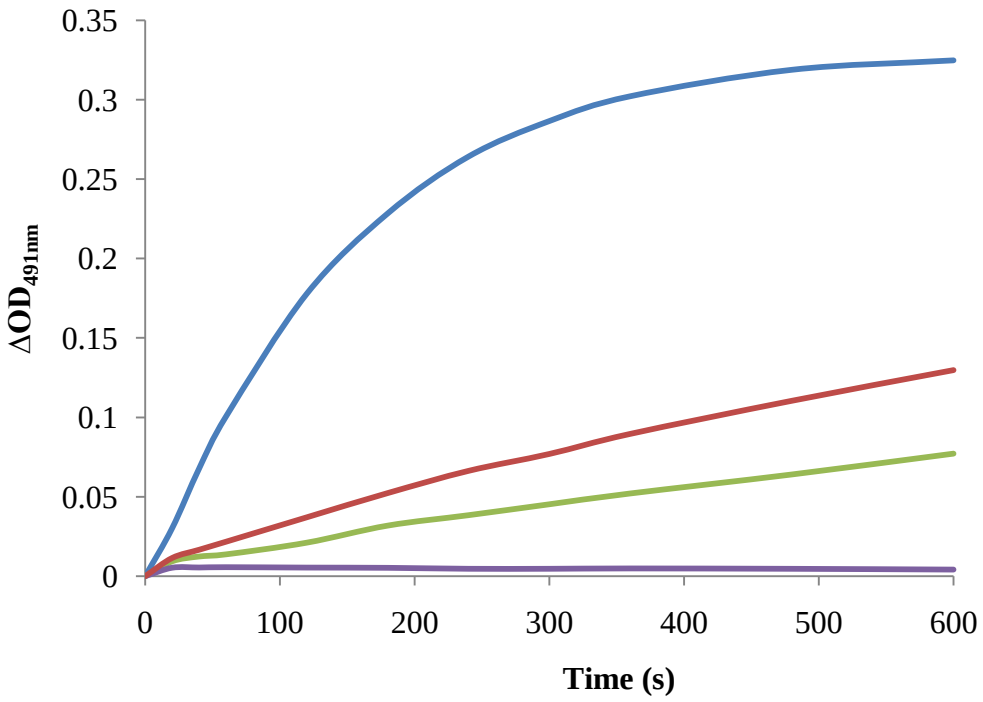

Figure 23: Activation of apo eSHMT by PLP in absence of 1mM MgATP; Activation of apo eSHMT by tightly bound PLP from ePL kinase-PLP-MgATP complex in absence (red line), and in presence of PLP-phosphatase (green curve). Activation of apo eSHMT by free PLP in absence (blue line), and in presence of PLP-phosphatase (purple line)

2.5 Conclusion: Cellular level of free PLP is regulated by combination of different mechanisms including activity of PLP-phosphatase and feed-back inhibition of PNP oxidase. This study also suggests feedback inhibition of PL kinase as another possible mechanism of PLP regulation. PLP inhibits PL kinase by binding to the active site and forming a non-productive ternary complex PL kinase-PLP-MgATP at K_i of 22.6 μM. Spectrophotometric and structural data showed that one molecule of PLP binds at the active site of the enzyme at each subunit. It remains tightly bound to the enzyme even after dialysis or after passing through a sizing column. The transfer studies also suggest strong possibility of channeling of PLP from PL kinase to PLP-dependent enzyme.

CHAPTER 3

CHARACTERIZE PROTEIN-PROTEIN INTERACTIONS BETWEEN PL KINASE AND B_6 ENZYMES

3.1 Introduction:

The experiments described in previous chapters suggest channeling or compartmentation to be a probable mechanism for PLP transfer from PL kinase to PLP-dependent enzymes. Nevertheless, conclusive proof for channeling mechanism requires that a physical complex forms between the kinase and B_6 enzymes. Association of proteins into supermolecules for transfer of substrates has been recognized for several years. Several biophysical and molecular biology methods are available to detect and quantify protein-protein interactions. These include but not limited to affinity chromatography, affinity blotting, immunoblotting, co-immunoprecipitation, fluorescence polarization (FP), and Surface Plasmon Resonance (SPR).[57] In our studies we used affinity chromatography and FP to determine whether PL kinase makes specific interaction with various B_6 enzymes, a pre-requisite for channeling mechanism.

Affinity chromatography, which provides qualitative measure of the interaction, employs a very simple approach to detect protein-protein interactions. It involves attachment of one of the interacting partner on solid support, from which non-specific proteins are readily washed off by buffer containing low salt concentration. The attachment can be done by using one of several approaches, such as affinity tagging, epitope tagging or employing fusion proteins. After immobilizing one of the interacting partners on solid support, the other partner or cell lysate is added on it. This added protein or any protein in the cell lysate, if interacts with the immobilized

protein, will also be immobilized on the solid support, while other non-specific proteins get washed off. The interacted proteins are co-eluted and analyzed to confirm the interaction.

Fluorescence polarization is a very sensitive technique for the quantification of protein-protein or protein-ligand interactions.[57, 60] The phenomenon of fluorescence polarization depends upon the rotational movement of fluorescent molecule. Any fluorescent molecule, having an absorption dipole parallel to the plane polarized light become excited by plane polarized light at its excitation wavelength. It remains in the excited state for certain time (termed fluorescent life-time, and ranges between one to ten nanoseconds) and return to ground-state while emitting light. During fluorescent life time, the excited molecule is prone to rotational movement, which decreases the chances of emitting the light parallel to the absorption dipole and thus results in relative depolarization of fluorescence intensity. The rotational movement, in turn, depends upon the molecular mass of the fluorescent molecule. Increase in molecular mass results in increase in polarization due to decrease in rotational movement during fluorescent life-time. This property makes this technique very useful in quantifying the protein-protein interactions, in which one of the interacting partners is fluorescently tagged. The availability of different fluorescent dyes, with fluorescence life-times ranging from one to ten nanoseconds, makes fluorescence polarization a very sensitive technique for quantifying protein-protein interactions for proteins between ten to hundreds of kilodaltons.[60]

3.2 Materials: Nickel nitriloaceticacid (NiNTA) slurry was purchased from QIAGEN (Valencia, CA). Fluorescein-5-maleimide was purchased from Invitrogen (Eugene, OR). The Corning 96-well plates (model 3792) were purchased from Sigma Aldrich (St. Louis, MO). Glycogen phosphorylase b was purchased from Sigma Aldrich (St. Louis , MO). All the proteins were purified as described previously. Centrifugal filter devices were obtained from Milipore (Bedford, MA).

3.3 Methods

3.3.1 Preparation of enzyme solutions: Purity of all the proteins was judged by SDS PAGE. All the proteins were concentrated using Centricon-YM 30 filter devices (MWCO 30 kDa) and dialyzed against 20 mM Sodium BES, pH 7 for use in affinity chromatography experiment, while for fluorescence polarization, they were dialyzed against 50 mM HEPES buffer, pH 7.55 containing 150 mM KCl and 0.01% Triton. The proteins were quantified by recording OD_{280nm} using their extinction co-efficient as previously reported.[4, 55, 73]

3.3.2 Activity analyses of purified enzymes: All the purified enzymes were analyzed for their activity as per the procedures described in previous chapter.

3.3.3 Characterization of protein-protein interactions using affinity chromatography: The two proteins were mixed in 1:1 stoichiometry. 1 mg of protein mixture was taken and diluted to 100 µL with 20 mM sodium BES buffer, pH 7. This protein mixture was loaded on NiNTA column, pre-equilibrated with 50 mM monobasic sodium phosphate, pH 8 containing 300 mM NaCl and 5 mM imidazole. The bed volume of column was 500 µL. After loading the mixture, the column was washed thoroughly with the equilibration buffer (washing buffer). Fractions of 400 µL were collected and analyzed for protein content by recording

OD_{280nm}. The column was washed till no protein came out, as observed from OD_{280nm}. After washing, bound protein was eluted by 50 mM monobasic sodium phosphate, pH 8 containing 250 mM imidazole and 300 mM NaCl (elution buffer). Protein elution was monitored by recording OD_{280nm}. Control experiments were also run, in which individual proteins, i.e. hPL kinase and rcSHMT were loaded on NiNTA column. Fractions for washing and elution were collected in similar fashion. Finally, the fractions for washing and elution for hPL kinase, rcSHMT and hPL kinase + rcSHMT were analyzed by SDS-PAGE.

3.3.4 Preparation of labeled PL kinase with Fluorescein-5-maleimide: For quantification of the protein-protein interactions, we used fluorescence polarization technique, and this section describes the tagging of PL kinase with fluorescein-5-maleimide for this study. Fluorescein-5-maleimide tags the protein via reacting with the –SH present on proteins. For tagging PL kinase, fluorescein-5-maleimide (1 mM) was mixed with 50 µM PL kinase in 1 mL of 50 mM sodium HEPES buffer, pH 7.55 containing 150 mM KCl and 0.01% Triton. The reaction was allowed to proceed overnight at 4°C in the dark. The reaction mixture was then centrifuged to remove any precipitate. The supernatant was dialyzed extensively against the same buffer in dark. The degree of labelling was determined by using equation 2. Catalytic activity of the protein was assessed before and after labelling by the assay described in chapter 2, section 2.2.3, to determine if labelling interferes with the activity of ePL kinase.

$$Moles\ fluor\ per\ mole\ protein = \frac{A_{max}\ of\ the\ labelled\ protein}{\varepsilon' * protein\ concentration\ (M)} * dilution\ factor \quad \ldots (2)$$

A_{max} is A_{495} and ε' is the molar extinction coefficient of FMI, which is 68,000 M^{-1} cm^{-1}.

3.3.5 Quantification of protein-protein interactions using fluorescence polarization (FP): *Corning* 96-well plates (model 3792) were used to carry out the FP measurements to quantify the interactions between ePL kinase and the following B6 enzymes, *E. coli* L-threonine aldolase (eL-TA), *E. coli* aspartate aminotransferase (eAAT), *E. coli* serine hydroxymethyltransferase (eSHMT), rabbit cytosolic serine hydroxymethyltransferase (rcSHMT) and glycogen phosphorylase b (GlyPb) from rabbit muscle. The tagged PL kinase (1 μM) was titrated with increasing concentrations of the B_6 enzymes mentioned above. The concentrations of PLP-dependent enzymes were varied from 1μM to 50 μM. Polarization measurements were conducted using *Tecan Polarion* polarimeter. The excitation wavelength and emission wavelengths were set at 495 nm and 535 nm respectively. The polarization values (in mP) were directly read from *Microsoft Excel* spreadsheet interfaced with the polarimeter. These obtained polarization values were plotted against concentrations of PLP-dependent enzymes. The dissociation constants for the protein-protein complexes were obtained by fitting the curves to equation 3 using *Sigmaplot 11*;

$$P_{obs} = \frac{(P_0 * K_d + 2P_{max} * [E])}{(K_d + 2[E])} \ldots\ldots\ldots (3)$$

Where, P_{obs} is the observed polarization value, P_0 is the polarization value when no PLP-dependent enzyme was added, P_{max} is the maximum polarization value obtained upon saturation of the polarization curve , K_d is the dissociation constant for the protein-protein complex and *[E]* is the concentration of PLP-dependent enzymes.

The above equation was derived from the equation 4[61] by assuming the equilibrium; *FMI-PLK* + *E* ⟷ *FMI-PLK -E*; where *FMI-PLK* is the tagged PL kinase with FMI (fluorescein-5-maleimide) and *E* is the PLP-dependent enzyme.

$$P_{obs} = \frac{([FMI - PLK] * P_{FMI-PLK} + [FMI - PLK - E] * P_{FMI-PLK-E})}{([FMI - PLK] + [FMI - PLK - E])} \ldots\ldots\ldots (4)$$

where, P_{obs} is the observed polarization values, $P_{FMI\text{-}PLK}$ is polarization intensity of tagged PL kinase, $P_{FMI\text{-}PLK\text{-}E}$ is the polarization values of the complex of tagged PL kinase and PLP- dependent enzyme, when all the PL kinase is in the complexed form. *[FMI-PLK]* and *[FMI-PLK-E]* are the concentrations of uncomplexed and complexed tagged-PL kinase respectively.

3.4 Results and Discussion:

3.4.1 Affinity chromatography for detection of protein-protein interactions: In our study, human PL kinase, with 6x-His tag on the N-terminal, provided a very easy way to immobilize it on NiNTA column. In this experiment, rcSHMT was not His-tagged, nevertheless if interaction occurs between hPL kinase and rcSHMT, it should result in immobilization of SHMT along with the PL kinase. The possible interaction between hPL kinase and rcSHMT was analyzed by loading 1:1 stoichiometric mixture of both enzymes on NiNTA column. Figure 24 shows the result of SDS-PAGE analysis of fractions obtained after washing (5 mM-30 mM) and elution (150 mM-250 mM) of NiNTA column loaded with hPL kinase alone (control), rcSHMT alone (control) and 1:1 stoichiometric mixture of hPL kinase and rcSHMT on the NiNTA column. Table 4 describes the results of the experiment.

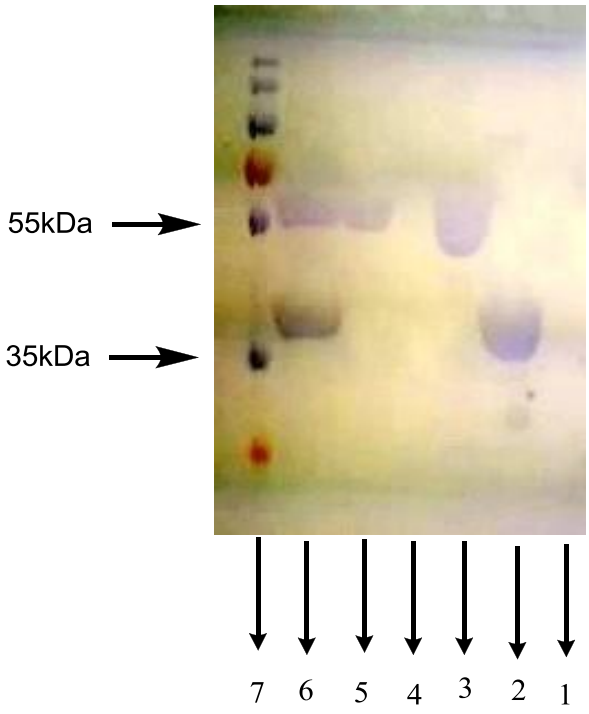

Figure 24: SDS-PAGE analysis of affinity chromatography eluates

Table 4: SDS-PAGE analysis of fractions eluted out after affinity chromatography analysis to detect interactions between hPL kinase and rcSHMT

Lane	Fraction		Result
1	Column loaded with hPL kinase alone	Washing	No protein came out
2		Elution	Protein eluted out
3	Column loaded with rcSHMT alone	Washing	rcSHMT got washed off from column
4		Elution	No protein was detected
5	Column loaded with 1:1 mixture of hPL kinase and rcSHMT	Washing	Some unbound rcSHMT got washed off
6		Elution	hPL kinase and rcSHMT got co-eluted
7	Protein marker		-

From Figure 24 (lane 1 and lane 2), it can be seen that hPL kinase was successfully immobilized on NiNTA. On the other hand, rcSHMT did not show any non-specific binding to the NiNTA matrix, as the rcSHMT, loaded alone on the column, was found to be completely washed off the column with the washing buffer (lanes 3 and 4). When both the proteins, i.e. hPL kinase and rcSHMT were loaded together on column, it was found out that some of the rcSHMT got washed off, while the major fraction of rcSHMT, which remained bound to hPL kinase, was co-eluted along with hPL kinase. Similar experiment was conducted with lysozyme as a control, in place of rcSHMT. The result (not displayed here) showed no interaction between hPL kinase and lysozyme. This clearly suggests that PL kinase and SHMT interacts specifically with each other to form a complex. This further serves to support the idea of PLP channeling. The next step is the quantification of this protein-protein interaction, which we did by fluorescence polarization.

3.4.2: Fluorescence polarization (FP) to quantify protein-protein interactions: Our previous study using affinity chromatography showed that hPL kinase forms specific interaction with rcSHMT. Following the qualitative analysis of interaction by affinity chromatography, we used FP to quantify the interactions. For that we used *E. coli* PL kinase and several other PLP-dependent enzymes, including, *E. coli* L-threonine aldolase (eL-TA), *E. coli* aspartate aminotransferase (eAAT), *E. coli* serine hydroxymethyltransferase (eSHMT), rabbit cytosolic serine hydroxymethyltransferase (rcSHMT) and glycogen phosphorylase b (GlyPb) from rabbit muscle having molecular weights of 140 kDa, 90 kDa, 90.5 kDa, 220 kDa and 92 kDa respectively. All of these enzymes belong to fold-type I, except GlyPb which belongs to fold-type V of B_6 enzymes. The activity of PL kinase was not affected by the tagging. The interactions of PL kinase with eSHMT, eL-TA, eAAT, rcSHMT and GlyPb were analyzed and the results are shown in Figure 25;

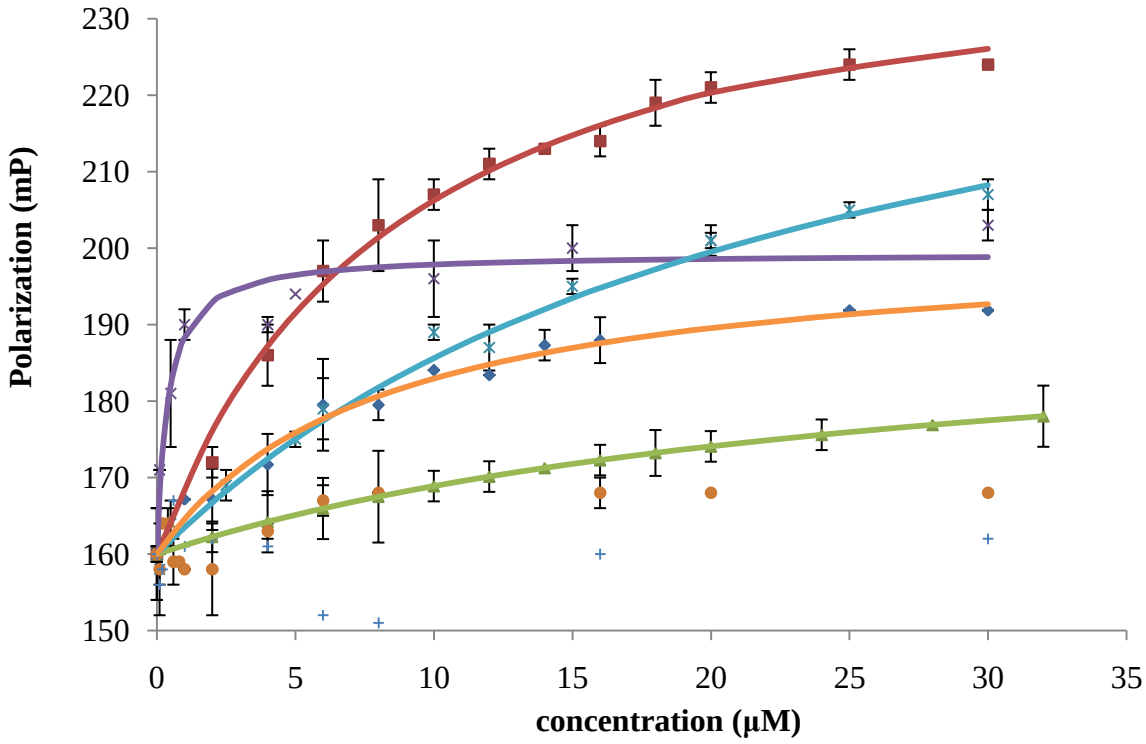

Figure 25: Fluorescence polarization titration; Change in fluorescence polarization intensity of FMI-PLK upon addition of increasing concentration of eSHMT (orange), eTA (light blue), eAAT (purple), rcSHMT (red) and Gly Pb (green) in 50 mM sodium HEPES, pH 7.55 containing 150 mM KCl and 0.01% Triton. Controls LDH (●) and lysozyme (+) were also run

A simple 1:1 model provided the best fit to the interactions, resulting in the K_d values that range from 0.4-50 µM, as noted in Table 5. Similar experiments by Cheung *et. al.* with PL kinase and pig alanine aminotransferase or glutamate decarboxylase resulted in K_d values 5-15 µM.[35, 47] Interestingly, GlyPb binding was found to be the weakest. It may be due to the fact that it is the most abundant B_6 enzyme in the body and the weak binding may act as control mechanism in order to prevent the GlyPb to out-compete all other apo B_6 enzymes. In the experiments, we used

lysozyme and lactate dehydrogenase (LDH, dimer;~140 kDa) as controls to show that non-B_6 proteins did not have any significant binding to PL kinase. The variation in polarization values between different PLP-dependent enzymes might be due to the difference in molecular weights between them.

Table 5: Affinity data for interactions of PL kinase with eSHMT, rcSHMT, eAAT, eTA and GlyPb

Enzyme	**Affinity (K_d)**
eSHMT	8 ± 1.2 μM
rcSHMT	8.4 ± 0.7 μM
eAAT	0.4 ± 0.01 μM
eTA	19 ± 2.8 μM
GlyPb	56 ± 8 μM

Fluorescence polarization data obtained for two different fold-types of PLP-dependent enzymes indicates that the binding between PL kinase and different PLP-dependent enzymes is specific. This data along with the binding data previously reported by Cheung *et. al.*[47] provides a very strong support to the argument of PLP channeling from PL kinase to PLP-dependent enzymes.

3.5 Conclusion:

The data obtained from both affinity chromatography and fluorescence polarization clearly indicates that PL kinase binds with PLP-dependent enzymes. This data along with results of the PLP transfer experiments indicate that channeling of PLP from PL kinase to PLP-dependent enzymes is a strong possibility.

CHAPTER 4

DETERMINE THE EFFECT OF PL KINASE S261F MUTATION ON ENZYME ACTIVITY AND STRUCTURE

4.1 Introduction: Several mutations on the genes coding for the B_6 salvage enzymes, PL kinase and PNP oxidase have been reported. In many of the cases, these mutations were found to be deleterious to health, because they lead to decrease in the enzyme activity.[18-20, 63-65] For PNP oxidase, many mutations have been linked to the fatal disorder, Neonatal epileptic encephalopathy.[19, 20, 63] Decrease in co-factor (FMN) binding affinity is found to be the cause of the decrease in activity in one of the mutant, R229W.[19] Similarly defective PL kinase has been reported in children suffering from autism.[64] In this study, we determined the effect of a single nucleotide polymorphism, causing S261F mutation, on human PL kinase activity. Single nucleotide polymorphism, by definition, occurs in at-least 1% of the population.[74] Hence, PL kinase, if affected by the S261F mutation, can lead to several disorders in large population carrying this SNP. This fact makes it essential to determine the effects of the mutation S261F on PL kinase's function and structure.

4.2 Materials: All culture media ingredients were purchased from Fischer Scientific (Pittsburgh, PA) or American Bioanalytical (Natick, MA). Nickel nitriloaceticacid (NiNTA) slurry was purchased from Qiagen (Valencia, CA). The QIAprep Spin Miniprep kit for plasmid isolation was purchased from Qiagen (Valencia, CA). The Quickchange Site-directed mutagenesis kit was purchased from Stratagene (La Jolla, CA). All the substrates were purchased from Sigma (St. Louis, MO). Centrifugal filter devices were obtained from Milipore (Bedford, MA).

4.3 Methods:

4.3.1 Site-directed mutagenesis: The recombinant plasmid containing gene *pdxK*, coding for PL kinase, inserted in pET 28a(+) was isolated by *Qiagen's QIAprep Spin Miniprep kit* as per the protocol described by *Qiagen*. Polymerase chain reaction was carried out as per the protocol given by *Stratagene*. The following primers were used to carry out polymerase chain reaction;

Forward primer: CAC CAC GTT CCA TTT GTG CCA GAA GAG

Reverse primer: GTG GTG CAA GGT AAA CAC GGT CTT CTC

The PCR product was transformed to *E. coli* XL-1 blue super-competent cells and transformants were grown on LB-agar media containing kanamycin (50 µg/mL) at 37°C. The following day, one colony was picked up and grown in 10 mL LB media, containing kanamycin (50 µg/mL), over night at 37°C. From this cell-culture, the plasmid, carrying the mutation, was isolated as described above. This plasmid was sent to VCU's DNA core facility for sequencing to confirm the mutation.

4.3.2 Optimization of expression condition for hPL kinase mutant (S261F): The mutant plasmid, after isolation from *E. coli* XL-1 blue supercompetent cells, was transformed to *E. coli* Rosetta (DE3) pLys cells for expression. The transformants were grown on LB-agar media containing kanamycin (50 µg/mL) and chloramphenicol (34 µg/mL), overnight at 37°C. The following day, one colony was picked up and grown in 10 mL LB-kanamycin-chloramphenicol media, overnight at 37°C and used to inoculate two separate 50 mL LB-kanamycin-chloramphenicol media. The cells were grown at 37°C until the OD_{600nm} reached to 0.8. The expression levels were analyzed at two different concentrations of β-isopropylthiogalactopyranoside (IPTG), i.e. 50 µM and 0.5 mM. The cells, induced with 0.5 mM

IPTG, were grown for additional 5 hours at 37°C; while the cells, induced with 50 μM IPTG, were grown for 24 hours at 18°C. After the induction period, cells were harvested by centrifugation and ruptured separately by high-pressure homogenization using *Avestin* cell disruptor. For determination of expression levels, 1 mL of cell-lysate was taken from both the mixtures and centrifuged. The supernatants containing soluble fraction of protein were collected. The cell pellets, containing protein in insoluble fraction, were re-suspended using suitable buffer. All of these fractions, containing protein in soluble, as well as, in insoluble forms were analyzed by SDS-PAGE.

4.3.3 Large scale expression and purification of mutant human PL kinase (S261F): The *E. coli* Rosetta (DE3) pLys cells containing the plasmid, carrying the mutation, were grown overnight at 37°C with shaking in 200 mL LB-kanamycin-chloramphenicol media. It was used to inoculate 4 L LB-kanamycin-chloramphenicol media the following morning. Cells were grown until OD_{600nm} reached to 0.8, induced with 50 μM β-isopropyl thiogalactopyranoside (IPTG), grown for additional 24 hours at 18°C and then harvested by centrifugation. Cell pellets were re-suspended in 150 mL cell-lysis buffer (50 mM NaH_2PO_4, pH 8 containing 300 mM NaCl and 10 mM imidazole). After re-suspension, the cells were ruptured by high-pressure homogenization using *Avestin* cell disruptor. Streptomycin sulfate was added to cell-lysate at concentration of 10 g/L to remove excess nucleic acids, which was then centrifuged to remove the precipitate and cell debris. The supernatant was decanted and loaded on NiNTA column, pre-equilibrated with lysis buffer. The column was washed thoroughly with lysis buffer until OD_{280nm} reached below 0.1, and further washed several times with the same buffer, containing higher concentrations of imidazole (10-75 mM). The enzyme was eluted from the column with 50 mM monobasic sodium phosphate, pH 8.0, containing 300 mM NaCl, and 150 mM

imidazole. Fractions containing protein of >95% purity, as judged by SDS-PAGE, were pooled together and concentrated by precipitation with 60% ammonium sulfate. The protein pellets were stored at -20°C for further usage.

4.3.4 Expression and purification of wild type PL kinase: The wild type PL kinase was expressed and purified as described in chapter 2 under section 2.3.1

4.3.5 Activity analysis of purified PL kinase S261F: The activity analysis of purified mutant enzyme was carried out as per the procedure described in chapter 2 under section 2.3.2 Activity analysis of wild type enzyme was also carried out in the same manner to compare its activity with the mutant enzyme. Comparison was made at two different concentrations of both enzymes, i.e. hPL kinase S261F and hPL kinase wild type.

4.3.6 Analysis of secondary structure: Secondary structural elements of wild-type and mutant enzyme were analyzed by recording circular dichroism (CD) spectra in a 0.5 cm cell at room temperature using *Olis* spectropolarimeter. The protein solutions were dialyzed against 20 mM potassium phosphate buffer, pH 7.2 and diluted to 0.1 mg/mL before analysis. All the spectra were blanked against buffer and recorded in range of 180 nm to 250 nm. The spectra were obtained in form of ellipticity vs. wave-length, which were normalized by converting ellipticity to Molar ellipticity by using equation 5.

$$\Theta = \Theta^0 * \frac{M}{c * l * n} \ldots\ldots\ldots (5)$$

Where, Θ = molar ellipticity, Θ^0 = observed ellipticity (in degrees), M = molecular weight, c = concentration, l = path-length of the cell and

n = *mean residual weight* = $\frac{molecular\ weight\ of\ protein}{number\ of\ amino\ acids}$

4.3.7 Tertiary structure analysis: Both wild-type and mutant enzymes, dialyzed against 20 mM potassium phosphate buffer, pH 7.24, were analyzed by fluorescence spectroscopy. The measurements were done in a 1 cm cell using *Shimadzu RF-5301* spectrofluorometer. The samples were excited at 295 nm and the emission-spectra were recorded between 300 to 400 nm, after blanking the spectrofluorometer against buffer. The slit-width was adjusted at 7.5 mm and all the measurements were done at room temperature.

4.3.8 Oligomerization state analysis: To check the oligomerization state, both mutant and wild-type enzymes were analyzed by native-PAGE. About 10 µL of each enzyme were mixed with 10 µL of native sample buffer and loaded on native gel. The gel was prepared without denaturants (SDS). It was run at 15 volts for about 2 hours. The gel was stained and, after destaining, analyzed for band positions of both the mutant and the wild-type enzyme.

4.4 Results and Discussion:

4.4.1 Site-directed mutagenesis: The sequencing of isolated plasmid, carrying the mutation, was performed at DNA core facility at VCU. It was done by using standard T7 promoter and T7 terminator primers. These primers were used for sequencing, as the vector pET28a(+) contained the T7-promoter and terminator sequences. The obtained sequence data was read in Applied Biosystem's sequence viewer and it confirmed the mutation S261F.

4.4.2: Optimization of expression condition for hPL kinase S261F: The main goal of expression condition optimization was to obtain the condition at which maximum amount of protein can be expressed to carry out further studies. The expression levels were analyzed at two different concentration of IPTG, which serves to induce protein production by bacteria. In one condition, IPTG was added to a concentration of 0.5 mM and cells were grown at 37°C, while in second condition, IPTG was added to a concentration of 50 μM and cells were grown at 18°C. The first condition is for fast induction, while the second is for slow induction. Slow induction, in some cases, may help in getting more soluble yields of protein due to more available folding opportunities during a slower process. In our case, both the conditions were analyzed before large-scale production. Figure 26 shows the result of analysis;

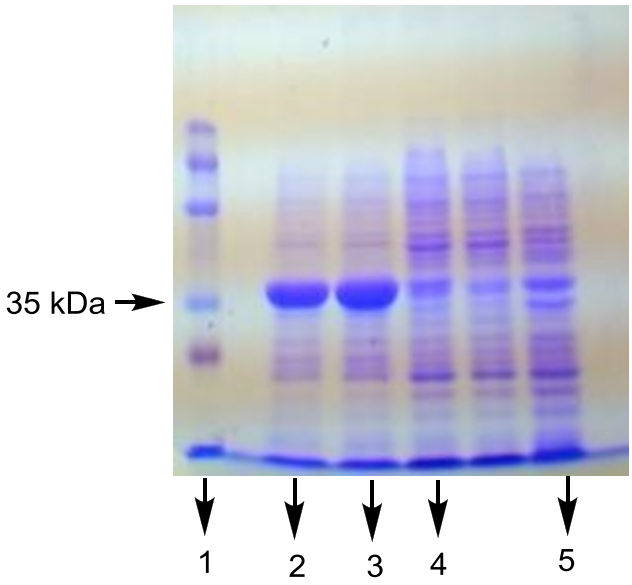

Figure 26: SDS-PAGE analysis for expression condition optimization of hPL kinase S261F; lane 1 corresponds to protein-marker, lane 2 and 3 correspond to protein in insoluble fractions for protein expressed at 37°C and 18°C respectively while lane 4 and 5 corresponds to the soluble fractions for 37°C and 18°C , respectively

As shown in Figure 26, the level of expression was slightly greater at 18°C, when low IPTG concentration was used. Therefore, the condition of low temperature with low IPTG concentration was used for large-scale protein-expression.

4.4.3 Large-scale expression and purification of human PL kinase S261F: The protein contained 6x-His tag at its N-terminal. Hence, purification, after cell-lysis, was performed by loading the cell-lysate on NiNTA column. Figure 27 shows the purification profile for hPL kinase S261F, and shows the enzyme purified to homogeneity, which was suitable for all further studies.

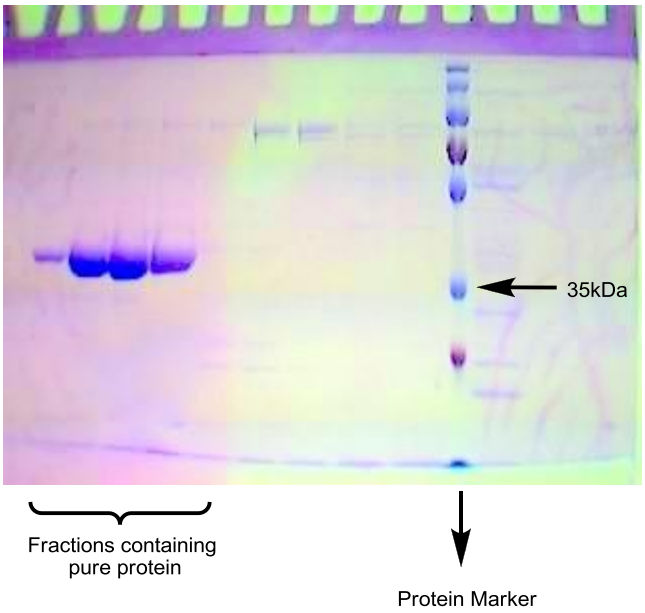

Figure 27:Purification profile of hPL kinase S261F; SDS-PAGE analysis of fractions eluted from NiNTA column when the column was washed with 50 mM NaH_2PO_4 containing 300 mM NaCl and 150 mM Imidazole

4.4.4 Activity analysis: The enzymatic activity of the mutant and wild-type were studied and compared. Table 6 shows the result of that analysis;

Table 6: Activity comparison of hPL kinase S261F and wild-type hPL kinase at two different concentrations of enzymes

Enzyme concentration (mg/mL)	**Rate (min^{-1})**	
	Wild-type	**Mutant**
0.1	0.0275 ± 0.006	0.0235 ± 0.01
0.2	0.0492 ± 0.015	0.0524 ± 0.012

This analysis indicated that both the proteins were equally active and mutation had no effect on activity of protein. On the basis of this study, in-depth kinetic analysis was not pursued.

4.4.5 Secondary structure analysis: Circular Dichroism is a sensitive technique for characterization of protein structure. It can readily detect any change in protein structure.[83] Figure 28 shows the spectra for both proteins;

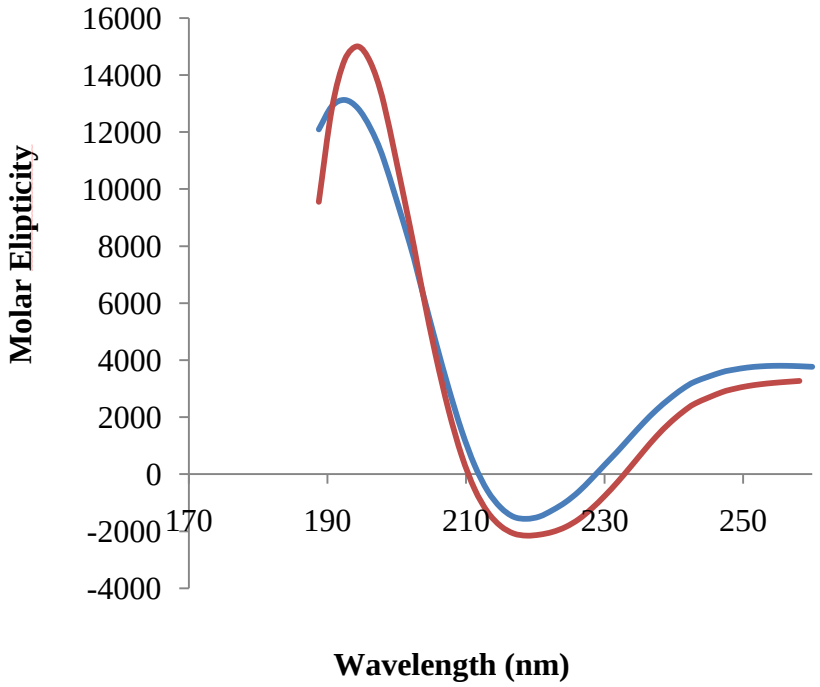

Figure 28: Secondary structure comparison; CD spectra of both hPL kinase wild-type (blue) and hPL kinase S261F (red)

The Far UV-CD spectra for both, wild-type and mutant enzymes were found to resemble each other, which suggest that the proteins have similar secondary structures; thus the mutation was not found to have any obvious effect on the secondary structure.

4.4.6 Tertiary structure analysis: Tertiary structures of the mutant, with the wild type as a control, were analyzed using fluorescence spectroscopy, by exciting the proteins at 295 nm and recording the emission spectra between 300-400 nm. This analysis employs the property of tryptophan residues, which have excitation maximum at 295 nm. Depending upon their local environment, characteristic emission spectrum with maximum between 308-355 nm is obtained. Any change in structure of protein and hence environments of tryptophan residues can change the spectrum also.[76] Therefore, the comparison of spectra of wild-type and mutant hPL kinase can yield valuable information regarding the structural change, if any.

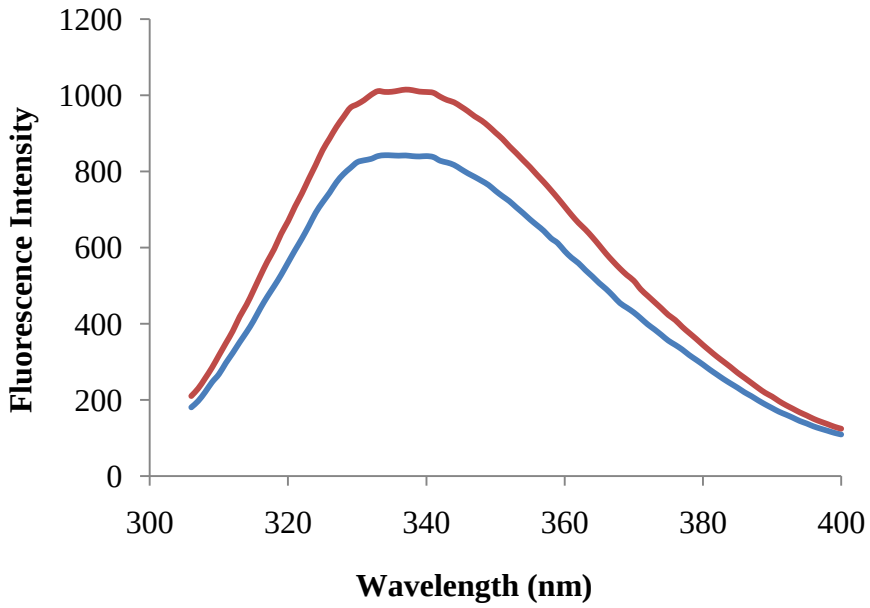

Figure 29: Tertiary structure comparison; Fluorescence emission spectra for hPL kinase wild-type (red) and hPL kinase S261F (blue)

Figure 29 shows the fluorescence spectra for both the hPL kinase wild-type and hPL kinase S261F, which indicates a slight decrease in the emission maximum as compared to wild-type enzyme, but no shift of the maximum was noticed. The decrease in emission maximum could be due to a slight variation in protein concentrations because of difference in purity of both the enzymes. The result however shows that the tertiary structures of both the proteins are almost similar. The S261F mutation is probably not altering the structure and hence the function of hPL kinase.

4.4.7 Oligomerization state analysis: The oligomerization state of the mutant with the wild type as a control was analyzed using Polyacrylamide gel electrophoresis (PAGE) under native conditions. The native PAGE separates the proteins depending on their molecular weights. Figure 30 shows native-PAGE analysis for both hPL kinase wild-type and hPL kinase S261F;

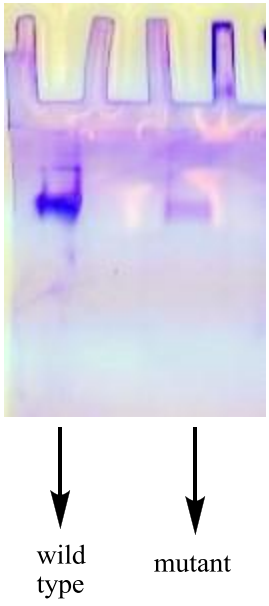

Figure 30: Oligomerization state comparison; native PAGE analysis of hPL kinase wild-type and hPL kinase S261F

Figure 30 clearly indicates that hPL kinase S261F is in identical oligomerization state as the wild-type enzyme and mutation is probably not affecting the quaternary structure as well.

4.5 Conclusion: The effect of a Single Nucleotide Polymorphism in gene *pdxK*, coding for PL kinase S261F was analyzed. The mutant protein was successfully expressed and purified to homogeneity. This mutant was compared with the wild-type enzyme for its catalytic activity, as well as, secondary, tertiary and quaternary structures. In all aspects, it was found to be identical with wild-type enzyme. The results show that this SNP (S261F) in *pdxK* might not have any pathological implications.

CHAPTER 5

DETERMINE THE EFFECT OF GINKGOTOXIN ON PL KINASE ACTIVITY AND STRUCTURE

5.1 Introduction: For a very long time *Ginkgo biloba* has been considered as an important therapeutic agent. It is even considered sacred in some parts of the world because of its presumed therapeutic property. In mainland China and Japan, as well as several parts of the world, preparations from *Ginkgo biloba* are used to treat conditions such as, insufficiency of blood-flow, cerebral insufficiency, memory deficit, lack of concentration, depression, dizziness, tinnitus, vertigo and headaches, bronchial asthma, irritable bladder, cough and even alcohol abuse.[28] Several clinical trials have also been reported for various preparations of *G. biloba*, but these studies have always resulted in controversial outcomes.[28] Several reports for detailed analysis of *G. biloba*'s constituents have been published and they have identified an array of different constituents, including ginkgotoxin, also known as 4'-O-methylpyridoxine .[29, 30] Apart from *G. biloba*, Ginkgotoxin is also found to be present in *Albizzia* species.[66] Ginkgotoxin, as the name suggests, is a potent neurotoxin. Toxicity occurs due to over-dose of any medicinal preparation from *G. biloba* or by ingestion of seeds, which are used in diet in Japan, as well as in China.[30, 65] Toxicities associated with ginkgotoxin are characterized by symptoms such as seizures, tonic/clonic convulsions, vomiting and impaired consciousness, which disappear with administration of PLP.[27, 29] This led to the suggestion that ginkgotoxin may have inhibitory effect on PL kinase and/or PNP oxidase activities. Several studies have confirmed ginkgotoxin's inhibitory activity against the kinase, but not the oxidase.[27, 28, 77] However, it has been suggested that the phosphorylated form of ginkgotoxin could inhibit the oxidase activity. This means that *in*

vivo phosphorylation of ginkgotoxin by the kinase may act on the oxidase to inhibit its activity. We have carried out in-depth kinetic analysis for ginkgotoxin inhibition of PL kinase and also used structural studies to understand the molecular basis of the inhibition. .

5.2 Materials:

The ginkgotoxin used in this study was synthesized by Dr. Danso-Danquah Richmond at the Institute for Structural Biology and Drug Discovery, VCU.

5.3 Methods:

5.3.1 Expression and purification of human PL kinase: Human PL kinase was expressed and purified as described previously in chapter 2 under section 2.3.1. The purified protein fractions after the NiNTA column were pooled together. Ammonium sulfate was added to 60% saturation to precipitate the protein. The protein pellet after ammonium sulfate was stored at -20°C for further use.

5.3.2 Determination of kinetic parameters for inhibition of PL kinase by ginkgotoxin: The protein was dialyzed against 20 mM sodium BES buffer, pH 7. All the assays were done in a 1 cm thermo-stated cuvette using *Agilent 8451* spectrophotometer. The assay for pyridoxal kinase activity was done as described previously in chapter 2 under section 2.3.2. The initial velocity data were recorded under the kinetic mode. For determination of kinetic parameters for inhibition, it was assumed that ginkgotoxin, due to structural similarity with PL, binds at the PL site. To confirm that and to determine the K_i for inhibition, three different concentrations (25 μM, 50 μM and 75 μM) of the drug ginkgotoxin were used and PL kinase was analyzed for activity at variable concentrations of PL (20-100 μM). MgATP was used at concentration of 1 mM. The initial velocity data were recorded in duplicate. The reciprocal rate

data were plotted against reciprocal of PL concentrations to obtain Lineweaver-Burk plot. The type of inhibition and kinetic parameter for the inhibition were determined from the plot.

5.3.3 Crystallization of PL kinase along with ginkgotoxin: PL kinase was first dialyzed against 20 mM sodium BES buffer, pH 7 containing 200 mM NaCl and 5 mM β-mercaptoethanol. The obtained protein solution was then concentrated to 25 mg/mL by using Centricon YM-10 centrifugal filter device. The concentrated protein solution was finally dialyzed against 20 mM sodium BES buffer, pH 7 containing 150 mM NaCl and 5 mM β-mercaptoethanol.

Wild-type PL kinase has previously been crystallized using 100 mM Tris-HCl, pH 8.0, and 52% 2-methyl-2,4-pentandiol (MPD) and 2.5 mM MgSO4. Therefore, all the co-crystallization attempts of PL kinase (700 μM) with ginkgotoxin (2 mM) and MgATP (1 mM) were focused around this condition. MPD concentration was varied between 45-60%. Hanging-drop method was used for the crystallization. X-ray quality crystals were obtained at the condition with 48% MPD.

5.3.4 Data collection, integration and scaling: The crystal was cryo-protected in mother-liquor solution containing 1 mM MgATP and 2 mM ginkgotoxin and diffraction data collected at 100K using a Molecular Structure Corporation (MSC) X-Stream Cryogenic Crystal Cooler, a Rigaku IV ++ image plate detector, and a *Rigaku MicroMax-007* X-Ray source (copper) fitted with MSC Varimax Confocal optics operating at 40 kV and 20 mA. Detector distance was set at 135 mm and exposure time was set at 2 minutes for each of the three frames, for which data was collected to assign unit cell parameters. After determining cell parameters, a total of 240 oscillation frames were collected, each at six minutes of exposure time. The data was

collected from φ 45° to 165° with 0.5° variations within each frame. Cell parameter determination and integration and scaling of data was done by *d*trek* provided in *CrystalClear* program package by *Rigaku America Co*. Integration of data was done by setting the resolution from 30 Å to 2.05 Å.

5.3.5 Structure determination: The diffraction intensity data was first converted to structure factor using the CCP4 suite of programs.[82] The isomorphous structure of hPL kinase D235A mutant (pdb id 2FHX) was used as a starting model for structure determination. The bound MgATP, MPDs, waters and sulfates were omitted for refinements. All the refinements were done using CNS (Crystallographic and NMR systems) program.[78] Rigid body refinement, conjugate gradient minimization, simulated annealing and B-factor refinements were performed. This led to identification of ginkgotoxin density at the PL site of both the subunits. MgATP density was also identified at both subunit active sites. The graphic programs, TOM[79] and COOT (Crystallographic object-oriented tool-kit)[80] were used for manual model adjustment as well as including the ginkgotoxin, MgATP, water, sulfate, MPD to the model. Refinements with intermittent model rebuilding have resulted in the current R_{free}/R_{work} of 28.3/25.4. Further refinement is ongoing. The data collection statistics and refinement parameters are shown in Table 7.

Table 7: Data collection statistics and refinement parameters for the structure of human PL kinase bound with ginkgotoxin

Data collection statistics	
Space group	I222
Unit cell a, b, c (Å)	92.75, 115.22, 169.55
Resolution range (Å)	28.81-2.10 (2.18-2.10)
Total number of reflections	186720
Number of unique reflections	49278
Average redundancy	3.79 (3.84)
% completeness	92.5 (92.3)
Output <I/ Σ(I)>	16.5 (8.3)
R_{merge}[a]	0.075 (0.288)
Refinement Statistics	
R_{free} *(%)*[b]	28.3
R_{work} *(%)*[c]	25.4
Average B (Å^2)/No. of non-H atoms	
Protein	40.4
Water	33
MPD	72.8
Anion	97.1
Cation	39.6
ATP	33.3

Numbers in parentheses refer to the outer (highest) resolution shell

[a] $R_{merge} = \Sigma|I - \langle I \rangle| / \Sigma(I)$, where I is the observed intensity and $\langle I \rangle$ is the weighted mean of the reflection intensity

[b] $R_{work} = \Sigma||Fo| - |Fc|| / \Sigma|Fo|$, where Fo and Fc are the observed and calculated structure factor amplitudes, respectively

[d] R_{free} is the crystallographic R_{work} calculated with 5 % of the data that were excluded from the structure refinement

5.4 Results and Discussion:

5.4.1 Determination of kinetic parameter for hPL kinase inhibition: Ginkgotoxin was tested for its inhibitory effects on hPL kinase. It was found to potently inhibit enzyme's activity with K_i of 18 μM. The Lineweaver-Burk plot also suggests the inhibitory effect of ginkgotoxin to be competitive with the substrate PL.

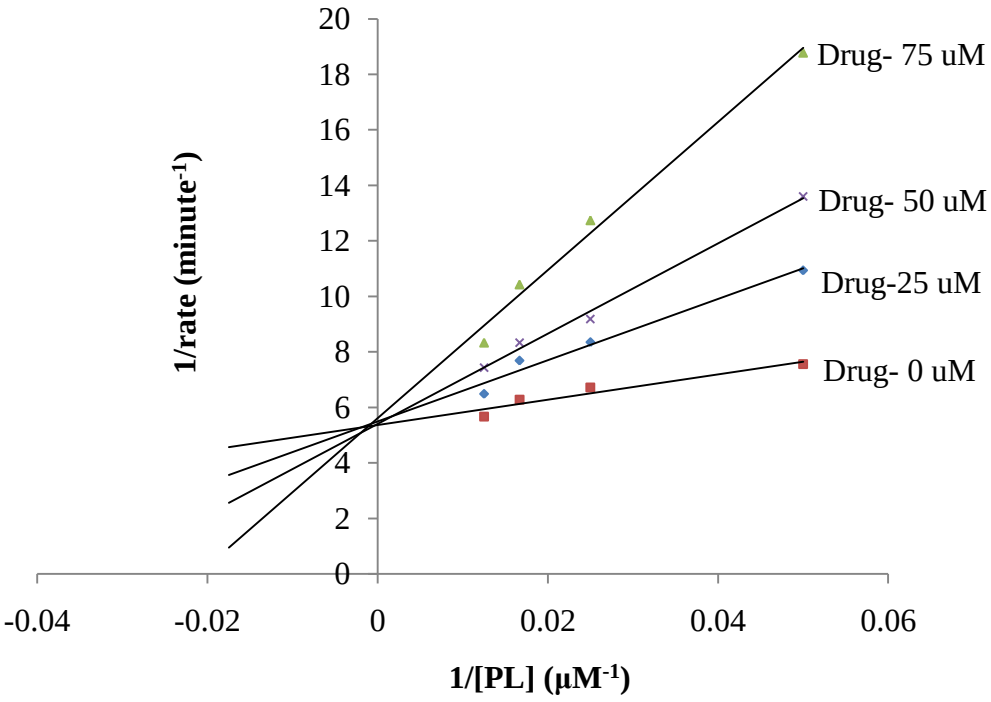

Figure 31: Lineweaver-Burk plot for characterization of Ginkgotoxin inhibition on hPL kinase

The study shows that Ginkgotoxin competitively inhibits PL binding, resulting in decrease in the metabolism of PL to PLP. Deficiency of PLP could potentially lead to disruption of the functions of several PLP-dependent enzyme activities causing neurotoxic effect. The competitive inhibition also suggests that ginkgotoxin is binding at the PL site of the enzyme.

5.4.2 Structure of ginkgotoxin bound at PL kinase: Based on the kinetic studies that suggested ginkgotoxin may be binding at the PL binding site, we undertook structural studies to confirm this and also to explain on atomic level how this compound inhibits the kinase. Co-crystals of PL kinase-ginkgotoxin were obtained with a minor modification of a previously reported crystallization condition for the wild type enzyme.[6] The structure was determined to a resolution of 2.1 Å. The current model contains 2 ginkgotoxin molecules, 2 ATP molecules, 2 each of Na^{+} and Mg^{2+}, 125 water, 6 sulfate and 6 MPD molecules. Both active sites have bound ginkgotoxin that closely superimpose on the substrate, PL. Figure 32 shows the dimeric PL kinase structure with bound MgATP and ginkgotoxin. The detailed PL kinase structure as well as the active site structure of PL kinase has previously been described.[6]

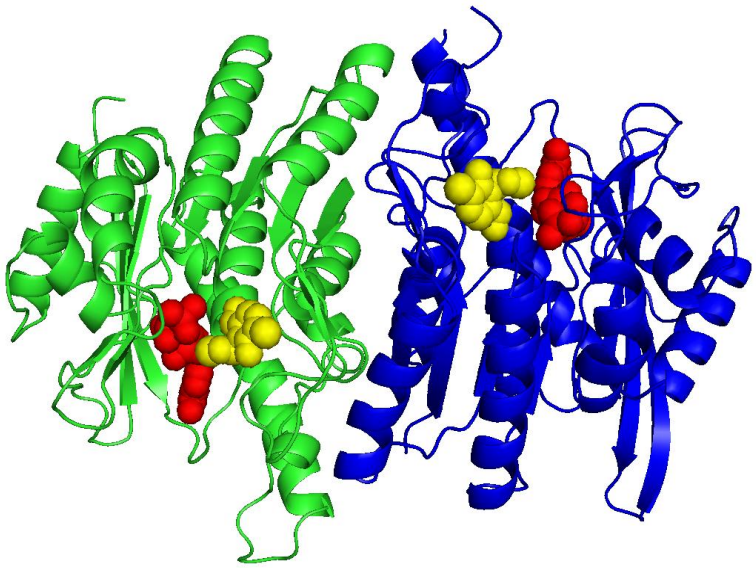

Figure 32: Dimeric structure of human PL kinase bound with ginkgotoxin and ATP; shown as spheres in yellow and red respectively. Monomer A and B are shown in green and blue respectively.

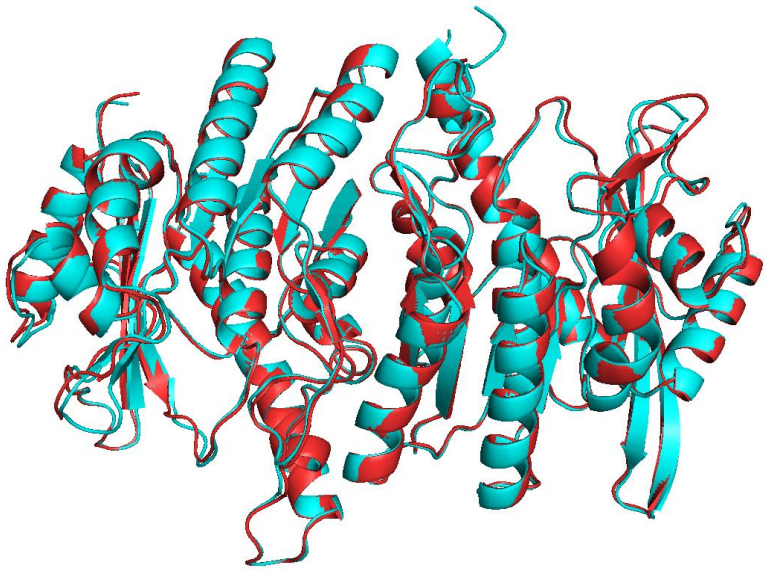

Figure 33: Superposition of human PL kinase (unliganded) and human PL kinase (inhibitor- bound); shown in red and cyan respectively

Figure 33 shows superposition of human PL kinase (unliganded) and human PL kinase with ginkgotoxin. The rmsd for the superposition was 0.4 Å, and shows that binding of ginkgotoxin to PL kinase does not have a significant effect on the overall conformation of PL kinase dimeric structure.

Each monomer of PL kinase has a unique active site that binds ATP, Mg^{2+} and Na^{+} molecules, as well as a ginkgotoxin. The mode of ginkgotoxin binding is shown in Figure 34, which is similar to those described for previously published binary complexes of PL kinase with bound PL.[5]

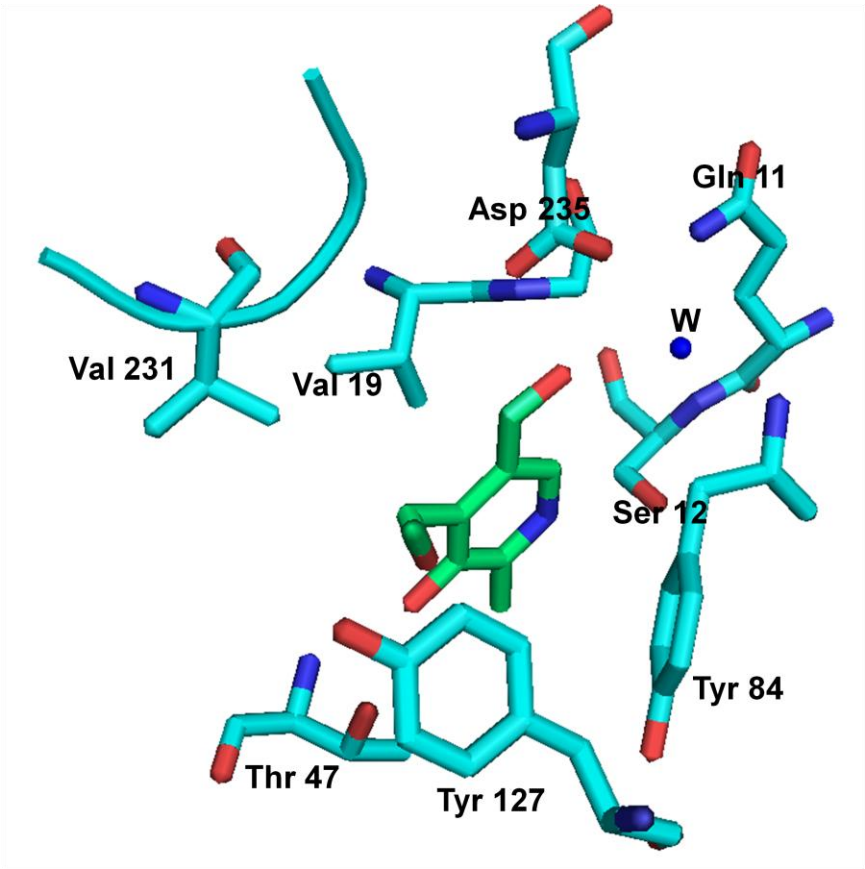

Figure 34: Binding of ginkgotoxin at the active-site of PL kinase

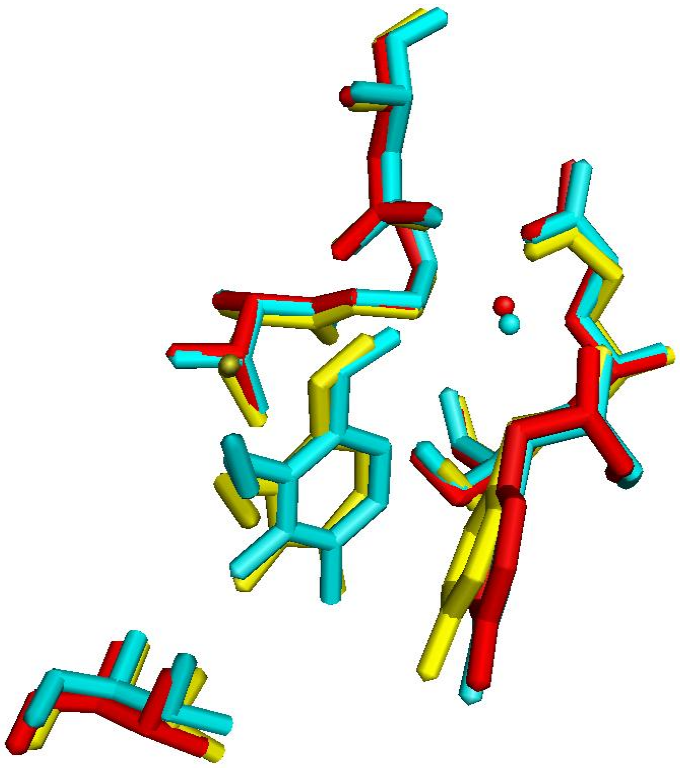

Figure 35: Superposition of human PL kinase (unliganded), sheep brain PL kinase (PL bound) and human PL kinase (inhibitor-bound) shown in red, yellow and cyan respectively

Figure 35 also shows superposition of the active-sites of human PL kinase (unliganded), human PL kinase- ginkgotoxin complex, and sheep brain PL kinase-PL complex. The structural comparison shows that ginkgotoxin binds in a similar fashion as pyridoxal, without any gross change in the active site structure. As expected, the interactions associated with PL binding are conserved with ginkgotoxin binding. These include a hydrogen-bond interaction between O_3 of ginkgotoxin and the main-chain nitrogen of Thr47; between N_1 of ginkgotoxin and the –OH

group of Ser12; between the hydroxyl of the 5'–CH_2OH and the carboxylate of Asp235. Theophylline and roscovitine, known inhibitors of PL kinase, are also known to inhibit PL kinase by binding to PL site of PL kinase, interacting with the same residues described above.[26] There are two unique interactions, that are absent in the PL binding complex, which may serve to explain the high affinity of ginkgotoxin to PL kinase. The 4'-O-methyl substituent of ginkgotoxin, which is absent in PL, is found to be located between and forming hydrophobic interactions with the protein residues Tyr127 and Val231. Also, 5'–CH_2OH of ginkgotoxin is involved in hydrogen-bond interaction with a nearby water molecule, which is held in position by hydrogen-bond interactions with the nearby Gln12 and Asp235. Although this water molecule is present in the unliganded PL kinase, it may possibly be playing structural role in ginkgotoxin binding.

5.4 Conclusion: Detailed kinetic analysis of ginkgotoxin's inhibition of PL kinase activity was carried out. It was found to inhibit PL kinase with a K_i of 18 μM, which is lower than the reported K_m of 30 μM for PL. From the kinetic analysis it was found to be a competitive inhibitor of the substrate PL. The X-ray crystallographic structure of PL kinase-ginkgotoxin complex shows that ginkgotoxin bind at the PL site of each subunit without any gross change in protein conformation, but with additional protein interactions. This data gave an insight into the mechanism of ginkgotoxin inhibitory activity. The structural studies also suggest that the 5'–CH_2OH could easily be phsophorylated by the enzyme which can act on the oxidase to inhibits activity.

Literature cited

1. Spinneker, A.; Sola, R.; Lemmen, V.; Castillo, M. J.; Pietrzik, K.; Gonzalez-Gross, M. Vitamin B_6 status, deficiency and its consequences- an overview. *Nutr. Hosp.*, **2007**, *22*, 7-24
2. Coburn, S. P; Slominski, A.; Mahuren, J. D.; Wortsman, J.; Hessle, L.; Millan, J. L. Cutaneous metabolism of vitamin B_6. *J. Invest Dermatol.*, **2003**, *120*, 292-300
3. McCormick, D. B., and Chen, H. Update on interconversions of vitamin B_6 with its coenzyme. *J. Nutr.*, **1999**, *129*, 325-327
4. diSalvo, M. L.; Hunt, S.; Schirch, V. Expression, purification, and kinetic constants for human and *Escherichia coli* pyridoxal kinases. *Protein expr. Purifi.*, **2004**, *36*, 300-306
5. Safo, M. K.; Musayev, F. N.; diSalvo, M. L.; Hunt, S.; Claude, J.; Schirch, V. Crystal structure of pyridoxal kinase from the *Escherichia coli pdxK* gene: Implications for the classification of Pyridoxal kinases. *J. Bacteriol.*, **2006**, *188*, 4542-4552
6. Musayev, F. N.; diSalvo, M. L.; Ko, T.; Gandhi, A. K.; Goswami, A.; Schirch, V.; Safo, M. K. Crystal structure of human pyridoxal kinase: Structural basis of M^+ and M^{2+} activation. *Protein Sci.*, **2007**, *16*, 2184-2194
7. McCormick, D. B.; Gregory, M. E.; Snell, E. E. Pyridoxal phosphokinase, I. Assay, distribution, purification and properties. *J. Biol. Chem.*, **1961**, *236*, 2076-2084
8. McCormick, D. B. and Snell, E. E. Pyridoxal phosphokinases II. Effects of inhibitors. *J. Biol. Chem.*, **1961**, *236*, 2085-2088
9. Yang, Y.; Tsui, H. T.; Man, T. K.; Winkler, M. E. Identification and function of the *pdxY* gene, which encodes a novel pyridoxal kinase involved in the salvage pathway of

pyridoxal 5'-phosphate biosynthesis in *Escherichia coli* K-12. *J. Bacteriol*, **1998**, *180*, 1814-1821

10. Safo, M. K.; Musayev, F. N.; Hunt, S. Crystal structure of the *pdxY* protein from *Escherichia coli*. *J. Bacteriol.*, **2004**, *186*, 8074-8082
11. Gandhi, A. K.; Ghatge, M. S.; Musayev, F. N.; Sease, A.; diSalvo, M. L.; Schirch, V.; Safo, M. K. Kinetic and structural studies of the role of the active site residue Asp of human pyridoxal kinase. *Biochem. Biophys. Res. Commun.*, **2009**, *381*, 12-15
12. Yang, E. S., and Schirch, V. Tight binding of pyridoxal 5'-phosphate to recombinant *Escherichia coli* pyridoxine 5'-phosphate oxidase. *Arch. Biochem. Biophys.*, **2000**, *377*, 109-114
13. Amadasi, A.; Bertoldi, M.; Contestabile, R.; Bettati, S.; Cellini, B.; diSalvo, M. L.; Voltattorni, C. B.; Bossa, F.; Mozzarelli, A. Pyridoxal 5'-phosphate enzymes as targets for therapeutic agents. *Curr. Med. Chem.*, **2007**, *14*, 1291-1324
14. Jansonius, J. N. Structure, evolution and action of vitamin B_6- dependent enzymes. *Curr. Opin. Struct. Biol.*, **1998**, *8*, 759-769
15. Grishin, N. V.; Phillips, M. A.; Goldsmith, E. J. Modelling of the spatial structure of eukaryotic ornithine decarboxylase. *Protein Sci.*, **1995**, *4*, 1291-1304
16. Schneider, G.; Kack, H.; Lindqvist, Y. The manifold of vitamin B_6 dependent enzymes. *Structure*, **2000**, *8*, R1-R6
17. Khayat, M.; Korman, S. H.; Frankel, P.; Weintraub, Z.; Hershckowitz, S.; Sheffer, V. F.; Elisha, M. B.; Wevers, R. A.; Faik-Zaccai, T. C. PNPO deficiency: an under diagnosed inborn error of pyridoxine metabolism. *Mol. Genet. Metab.*, **2008**, *94*, 431-434

18. Plecko, B., and Stockler, S. Vitamin B6 dependent seizures. *Can. J. Neurol. Sci.*, **2009**, *Suppl 2*: S73-7

19. Musayev, F. N.; diSalvo, M. L.; Saavedra, M. A.; Contestabile, R.; Ghatge, M. S.; Haynes, A.; Schirch, V.; Safo, M. K. Molecular basis of reduced pyridoxine 5'-phosphate oxidase activity in neonatal epileptic encephalopathy disorder. *J. Biol. Chem.*, **2009**, *284*, 30949-30956

20. Clayton, P. T.; Surtees, R. A. H.; DeVille, C.; Hyland, K.; Heales, S. J. R. Neonatal epileptic encephalopathy. *Lancet*, **2003**, *361*, 1614

21. Laine-Cessac, P.; Cailleux, A.; Allain, P. Mechanisms of the human erythrocyte pyridoxal kinase by drugs. *Biochem. Pharmacol.*, **1997**, *54*, 863-870

22. Delport, R.; Ubbink, J.; Serfontein, W. J.; Becker, P. J.; Walters, L. Vitamin B_6 nutritional status in asthma: the effect of theophylline therapy on plasma pyridoxal 5'-phosphate and pyridoxal levels. *Int. J. Vitam. Nutr. Res.*, **1988**, *58*, 67-72

23. Hahn, I. H., and Varney, S. Pyridoxine treatment for seizures induced by theophylline and isoniazid? *Vet. Hum. Toxicol.*, **1999**, *41*, 342

24. Glenn, G. M.; Krober, M. S.; Kelly, P.; McCarty, J.; Weir, M. Pyridoxine as therapy in theophylline-induced seizures. *Vet. Hum. Toxicol.*, **1995**, *37*, 342-345

25. Bach, S.; Knockaert, M.; Reinhardt, J.; Lozach, O.; Schmitt, S.; Baratte, B.; Koken, M.; Coburn, S. P.; Tang, L.; Jiang, T.; Liang, D.; Schachtele, C.; Lerman, A. S.; Carnero, A.; Galons, H.; Dierick, J.; Pinna, L. A.; Meggio, F.; Totzke, F.; Gray, N.; Wan, Y.; Miejer, L. Roscovitine targets, protein kinases and pyridoxal kinase. *J. Biol. Chem.*, **2005**, *280*, 31208-31219

26. Tang, L.; Li, M.; Cao, P.; Wang, F.; Chang, W.; Bach, S.; Reinhardt, J.; Fernandin, Y.; Galons, H.; Wan, Y.; Gray, N.; Meijer, L; Jiang, T.; Liang, D. Crystal structure of pyridoxal kinase in complex with roscovitine and derivatives. *J. Biol. Chem.*, **2005**, *280*, 31220-31229

27. Kastner, U.; Hallmen, C.; Wiese, M.; Leistner, E.; Drewke, C. The human pyridoxal kinase, a plausible target for ginkgotoxin from Ginkgo biloba, *FEBS J.*, **2007**, *274*, 1038-1045

28. Leistner, E., and Drewke, C. Ginkgo biloba and ginkgotoxin. *J. Nat. Prod.*, **2010**, *73*, 86-92

29. Wada, K.; Ishigaki, S.; Ueda, K.; Masakatsu, S.; Masanobu, H. An antivitamin B_6 , 4'-methoxypyridoxine, from the seeds of Ginkgo biloba L. *Chem. Pharm. Bull.*, **1985**, *33*, 3555-3557

30. Wada, K.; Ishigaki, S.; Ueda, K.; Take, Y.; Sasaki, K.; Sakata, M.; Masanobu, H. Studies on the constitution of edible and medicinalplants. I. isolation and identification of 4-O-methylpyridoxine , toxic principle from seed of Ginkgo bilobaL. *Chem. Pharm. Bull.*, **1988**, *36*, 1779

31. Cabantchik, I. Z.; Balshim, M.; Breuer, W.; Rothstein, A. Pyridoxal phosphate- an anionic probe for protein amino groups exposed on the outer and inner surfaces of intact human red blood cells. *J. Biol. Chem.*, **1975**, *250*, 5130-5136

32. Fenalti, G.; Law, R.; Buckle, A. M.; Langendorf, C.; Tuck, K.; Rosado, C. J.; Faux, N. G.; Mahmood, K.; Hampe, C. S.; Banga, P.; Wilce, M.; Schmidberger, J.; Rossjohn, J.; El-Kabbani, O.; Pike, R. N.; Smith, I.; Mackay, I. R.; Rowley, M. J.; Whisstock, J. C.

GABA production by glutamic acid decarboxylase is regulated by a dynamic catalytic loop. *Nat. Struct. Biol.*, **2007**, *14*, 280-286

33. Ishioka, N.; Sato, J.; Nakamura, J.; Ohkubo, T.; Takeda, A.; Kurioka, S. *In vivo* modification of $GABA_A$ receptor with a high dose of pyridoxal phosphate induces tonic-clonic convulsion in immature mice. *Neurochem. Int.*, **1995**, *26*, 369-373
34. Bartzatt, R., and Beckman, J. D. Inhibition of phenol sulfotransferase by pyridoxal phosphate. *Biochem. Pharmacol.*, **1994**, *47*, 2087-2095
35. Kim, Y. T.; Kwok, F.; Churchich, J. E. Interactions of pyridoxal kinase and aspartate aminotransferase emission anisotropy and compartmentation studies. *J. Biol. Chem.*, **1988**, *263*, 13712-13717
36. Choi, S.; Churchich, J. E.; Zaiden, E.; Kwok, F. Brain pyridoxine-5-phosphate oxidase: modulation of its catalytic activity by reaction with pyridoxal 5-phosphate and analogs. *J. Biol. Chem.*, **1987**, *262*, 12013-12017
37. Merrill, A. H.; Horiike, K.; McCormick, D. B. Evidence for the regulation of pyridoxal 5'-phosphate formation in liver by pyridoxamine (pyridoxine) 5'-phosphate oxidase. *Biochem. Biophys. Res. Commun.*, **1978**, *83*, 984-990
38. Kwon, O.; Kwok, F.; Churchich, J. E. Catalytic and regulatory properties of native and chymotrypsin treated pyridoxine-5-phosphate oxidase. *J. Biol. Chem.*, **1991**, *166*, 22136-11140
39. Jang, Y. M.; Kim, D. W.; Kang, T.; Won, M. H.; Baek, N.; Moon, B. J.; Choi, S. Y.; Kwon, O. S. Human pyridoxal phosphatase: molecular cloning, functional expression, and tissue distribution. *J. Biol. Chem.*, **2003**, *278*, 50040-50046

40. Zhao, G. and Winkler, M. E. Kinetic limitation and cellular amount of pyridoxine (pyridoxamine) 5'-phosphate oxidase of *Escherichia coli* K-12. *J. Bacteriol.*, **1995**, *177*, 883-891

41. Choi, J.; Bowers-Komro, D. M.; Davis, M. D.; Edmondson, D. E.; McCormick, D. B. Kinetic properties of Pyridoxamine (pyridoxine)-5'-phosphate oxidase from rabbit liver. *J. Biol. Chem.*, **1983**, *258*, 840-845

42. Cheng, Y., and Prusoff, W. H. Relationship between the inhibition constant (K_i) and the concentration of inhibitor which causes 50 percent inhibition (I_{50}) of an enzymatic reaction. *Biochem. Pharmacol.*, **1973**, *22*, 3099-3108

43. Boe, A. S.; Bredholt, G.; Knappskog, P. M.; Storstein, A.; Vedeler, C. A.; Husebye, E. S. Pyridoxal phosphatase is a novel cancer autoantigen in the central nervous system. *British Journal of Cancer*, **2004**, *91*, 1508-1514

44. Kwok, F.; Churchich, J. E. Interaction between pyridoxal kinase and pyridoxine-5-P oxidase, two enzymes involved in metabolism of vitamin B_6. *J. Biol. Chem.*, **1980**, *255*, 882-887

45. Lee, H.; Moon, B. J.; Choi, S. Y.; Kwon, O. S. Human pyridoxal kinase: overexpression and properties of the recombinant enzyme. *Mol. Cells*, **2000**, *10*, 452- 459

46. Li, M.; Kwok, F.; Wen-Rui, C.; Lau, C.; Zhang, J.; Lo, S. C. L.; Jiang, T.; Liang, D. Crystal structure of brain pyridoxal kinase, a novel member of the ribokinase superfamily. *J. Biol. Chem.*, **2002**, *277*, 46385-46390

47. Cheung, P.; Fong, C.; Ng, K.; Lam, W.; Leung, Y.; Tsang, C.; Yang, M.; Wong, M. Interaction between pyridoxal kinase and pyridoxal-5-phosphate dependent enzymes. *J. Biochem.*, **2003**, *134*, 731-738

48. Fu, T.; diSalvo, M. L.; Schirch, V. Distribution of B_6 vitamers in *Escherichia coli* as determined by enzymatic assay. *Anal. Biochem.*, **2001**, *298*, 314-321

49. Schirch, V.; Hopkins, S.; Villar, E.; Angelaccio, S. Serine hydroxymethyltransferase from *Escherichia coli*: Purification and properties. *J. Bacteriol.* **1985**, *163*, 1-7

50. diSalvo, M. L.; Fratte, S. D.; Biase, D. D.; Bossa, F.; Schirch, V. Purification and characterization of recombinant rabbit cytosolic serine hydroxymethyltransferase. *Protein Expr. Purif.*, **1998**, *13*, 177-183

51. Matthews, R. G., and Drummond, J. T. Providing one-carbon units for biological methylations: mechanistic studies on serine hydroxymethyltransferase, methylenetetrahydrofolate reductase, and methyltetrahydrofolate-homocysteine methyltransferase. *Chem. Rev.* **1990**, *90*, 1275-1290

52. Schirch, V., and Szebenyi, D. Serine hydroxymethyltransferase revisited. *Curr. Opin. Chem Biol.*, **2005**, *9*, 482-487

53. Stover, P., and Schirch, V. 5-formyltetrahydrofolate polyglutamates are slow tight binding inhibitors of serine hydroxylmethyltransferase. *J. Biol. Chem.*, **1991**, *266*, 1543-1550

54. Bhavani, S.; Trivedi, V.; Jala, V. R.; Subramanya, H. S.; Kaul, P.; Prakash, V.; Appajirao, N.; Savithri, H. S. Role of Lys-226 in the catalytic mechanism of Bacillus stearothermophillus serine hydroxymethyltransferase- Crystal structure and kinetic studies. *Biochemistry*, **2005**, *44*, 6929-6937

55. Cai, K., and Schirch, V. Structural studies on folding intermediates of serine hydroxymethyltransferase using single tryptophan mutants. *J. Biol. Chem.*, **1996**, *271*, 2987-2994

56. Schirch, V., and Gross, T. Serine transhydroxymethylase: identification as the threonine and allothreonine aldolase. *J. Biol. Chem.*, **1968**, *243*, 5651-5655

57. Phizicky, E. M., and Fields, S. Protein-protein interactions: methods for detection and analysis. *Microbiol. Rev.*, **1995**, *59*, 94-123

58. Spivey, H. O., and Ovadi, J. Substrate channeling. *Methods*, **1999**, *19*, 306-321

59. Miles, E. W.; Rhee, S.; Davies, D. R. The molecular basis of substrate channeling. *J. Biol. Chem.*, **1999**, *274*, 12193-12196

60. Lundblad, J. R.; Laurance, M.; Goodman, R. H. Fluorescence polarization analysis of protein-DNA and protein-protein interactions. *Mol. Endocrinol.*, **1996**, *10*, 607-612

61. Tompa, P.; Batke, J.; Ovadi, J.; Welch, G. R.; Srerej, P. A. Quantitation of the interaction between citrate synthase and malate dehydrogenase. *J. Biol. Chem.*, **1987**, *262*, 6089-6092

62. Bender, D. A., *Nutritional biochemistry of the enzymes*, 2nd edition, Cambridge University press: London, **2003**; pp 246- 250

63. Mills, P. B.; Surtees, R. A.H.; Champion, M. P.; Beesley, C. E.; Dalton, N.; Scambler, P. J.; Heales, S. J. R.; Briddon, A.; Scheimberg, I.; Hoffmann, G. F.; Zschocke, J.; Clayton, T. P. Neonatal epileptic encephalopathy in the PNPO gene coding pyridox(am)ine 5'-phosphate oxidase. *Hum. Mol. Genet.*, **2005**, *14*, 1077- 1086

64. Adams, J. B.; Frank, G.; Audhya, T. Abnormally high plasma levels of vitamin B_6 in children with autism not taking supplements compared to controls not taking supplements. *J. Altern. Complement. Med.*, **2006**, *12*, 59- 63

65. Kajiyama, Y.; Kenichi, F.; Hajime, T.; Yutaka, M. Ginkgo seed poisoning. *Pediatrics*, **2002**, *109*, 325- 327

66. Steyn, P. S.; Vleggar, R.; Anderson, L. A. P. Structure elucidation of two neurotoxins from *Albizia tanganyicensis*. *S. Afr. J. Chem.*, **1987**, *40*, 191- 2

67. Gropper, S. S.; Smith, J. L.; Groff, J. L. *Advanced nutrition and metabolism.* 5th edition, Wadsworth: Belmont, CA, **2009**; pp 364-369

68. Anonymous, Vitamin preparations as dietary supplements and as therapeutic agents. Council on scientific affairs. *JAMA*, **1987**, *257*, 1929-1936

69. Berger, A. R.; Schaumburg, H. H; Schroeder, C.; Apfel, S.; Reynolds, R. Dose response, coasting, and differential fiber vulnerability in human toxic neuropathy: a prospective study of pyridoxine neurotoxicity. *Neurology*, **1992**, *42*, 1367-1370

70. Alhadeff, L.; Gualtieri, C.; Lipton, M. Toxic effects of water-soluble vitamins. *Nutr. Rev.*, **1984**, *42*, 33-40

71. Elcock, A. H.; Potter, M. J.; Matthews, D. A.; Knighton, D. R.; McCammon, J. A. Electrostatic channeling in the bifunctional enzyme dihydrofolate reductase-thymidylate synthase . *J. Mol. Biol.*, **1996**, *262*, 370-374

72. Scarsdale, J. N.; Kazanina, J. N.; Radaev, S.; Schirch, V.; Wright, H. T. Crystal structure of rabbit cytosolic serine hydroxymethyltransferase. *Biochemistry*, **1999**, *38*, 8347-8358

73. Gill, S. C., vonHippel, P. H. Calculation of protein extinction co-efficients from amino-acid sequence data. *Anal. Biochem.*, **2001**, *298*, 314-321

74. Genome programs of the U.S. Department of Energy Office of Science. http://www.ornl.gov/sci/techresources/Human_Genome/faq/snps.shtml (accesed June 2010)

75. Engelborghs, Y., and Hellings, M. Time resolved protein fluorescence in multi-tryptophan proteins, In: *Methods in protein structure and stability analysis*, Uversky, V., and Permyakov, E., Eds.; Nova Science Publishers, Inc. **2007**, pp 237-256

76. Buss, K.; Drewke, C.; Lohmann, S.; Piwonska, A.; Leistner, E. Properties and interaction of heterologously expressed glutamate decarboxylase isoenzymes GAD65kDa and GAD67kDa from human brain with ginkgotoxin and its 5'- phosphate. *J. Med. Chem.*, **2001**, *44*, 3166- 3174

77. Salamon, N.; Gurgui, C.; Leistner, E.; Drewke, C. Influence of ginkgotoxin 5'-phosphate and depyridoxine 5'-phosphate on human pyridoxine 5'-phosphate oxidase. *Planta Med.*, **2009**, *75*, 563- 567

78. Brunger, A. T.; Adams, P. D.; Clore, G. M.; DeLano, W. L.; Gros, P.; Grosse-Kunstleve, R. W.; Jiang, J.; Kuszewski, J.; Nilges, M.; Pannu, N. S.; Crystallography & NMR systems: a new software suite for macromolecular structure determination. *Acta. Crytallogr. D*, **1998**, *54*, 905-921

79. Cambillau, C. and Horjales, E. TOM: a frodo subpackage for protein-ligand fitting with interactive energy minimization, *J. Mol. Graph.*, **1987**, *5*, 74-177

80. Emsley, P., and Cowtan, K. COOT: model-building tools for molecular graphics. *Acta. Crystallogr. D*, **2004**, *60*, 2126-2132

81. Lumeng, L.; Brasher, R. E.; Li, T. Pyridoxal 5'-phosphate in plasma. Source, protein-binding, and cellular transport. *J. Lab. Clin. Med.*, **1974**, *84*, 334- 343

82. Collaborative computational project, Number 4. The CCP4 suite: Programs for protein crystallography. *Acta. Crystallogr. D*, **1994**, *50*, 760-763

83. Towell, F. J., and Manning, M. C. Analysis of protein structure by circular dichroism. In *Analytical applications of Cicular Dichroism*, Purdie, N., and Brittain, H. G., Eds.; Elsevier: Amsterdam, **1994**; pp 175- 207